Large-Scale Modeling and Optimization of Routing, Modulation and Spectrum Assignment Problems in Optical Networks

Adham Mohammed

A Thesis

in

The Department

of

Mechanical, Industrial and Aerospace Engineering

Presented in Partial Fulfillment of the Requirements

for the Degree of

Master of Applied Science (Industrial Engineering) at

Concordia University

Montréal, Québec, Canada

December 2020

Concordia University

School of Graduate Studies

This is to certify that the thesis prepared

By: **Adham Mohammed**

Entitled: **Large-Scale Modeling and Optimization of Routing, Modulation and Spectrum Assignment Problems in Optical Networks**

and submitted in partial fulfillment of the requirements for the degree of

Master of Applied Science (Industrial Engineering)

complies with the regulations of this University and meets the accepted standards with respect to originality and quality.

Signed by the Final Examining Committee:

_____ Chair
Dr. Ivan Contreras

_____ External Examiner
Dr. Tse-Hsun (Peter) Chen

_____ Examiner
Dr. Ivan Contreras

_____ Supervisor
Dr. Brigitte Jaumard

Approved by _____
Martin Pugh, Chair
Department of Mechanical, Industrial and Aerospace Engineering

_____ 2021

_____
Mourad Debbabi, Interim Dean
Gina Cody School of Engineering and Computer Science

Abstract

Large-Scale Modeling and Optimization of Routing, Modulation and Spectrum Assignment Problems in Optical Networks

Adham Mohammed

One of the crucial decisions in managing flexible optical fiber networks is the provisioning of connection requests, known as the Routing and Spectrum Assignment (RSA) problem, and its extension: Routing, Modulation and Spectrum Assignment (RMSA) problem. Such problems are becoming more and more challenging everyday with the steadily increasing demand in optical networking. Therefore, considerable research effort has been exerted in developing models and algorithms to efficiently solve larger problem instances. Yet, there still exists a gap between the problem sizes that can be solved thanks to the previous research efforts and the realistic problem sizes. This work is one step forward towards reducing this gap.

In this thesis, we propose decomposition models for the RSA and RMSA problems based on lightpath configurations. The proposed models are Integer Linear Programs (ILPs) with an exponential number of configuration variables. Therefore, we have developed nested column generation algorithms to exactly solve both problems. Furthermore, Lagrangian Relaxation is used to compute valid upper bounds on the Integer Linear Programming (ILP) optimal objective values, in order to compute a measure of solution quality: the relative optimality gap.

The proposed algorithms are able to efficiently solve instances with sizes beyond what has been so far published in literature, and more importantly, with considerably higher quality, i.e., narrower relative optimality gaps.

Acknowledgments

To my beloved family..

Contents

List of Figures vii

List of Tables ix

1 Introduction 1

1.1 Background 1

1.2 Motivation 1

1.3 Contribution 2

1.4 Thesis Outline 2

2 Nested Column Generation Algorithm for the Routing and Spectrum Assignment Problem in Flexgrid Optical Networks 3

2.1 Introduction 3

2.2 Problem Statement 4

2.3 Mathematical Model 5

2.3.1 Master Problem 6

2.3.2 Higher-Level Pricing Problem 7

2.3.3 Lower-Level Pricing Problem 8

2.4 Solution Scheme 9

2.4.1 Nested Column Generation 9

2.4.2 Accuracy 9

2.5 Experimental Results 11

2.6 Conclusion 15

3 Nested Column Generation for Large-Scale Routing, Modulation and Spectrum Assignment in Flexible Optical Networks **16**

3.1 Introduction 16

3.1.1 Technical Background 17

3.1.2 Literature Review 17

3.1.3 Contribution 19

3.1.4 Paper Organization 19

3.2 Problem Statement 19

3.3 Mathematical Formulation 20

3.3.1 Lightpath Configuration-Based Decomposition 20

3.3.2 Mater Problem 21

3.3.3 Higher-Level Pricing Problem 24

3.3.4 Lower-Level Pricing Problem 25

3.4 Nested Column Generation 26

3.4.1 Higher-Level Column Generation 27

3.4.2 Lower-Level Column Generation 28

3.4.3 Accuracy 28

3.4.4 Lagrangian Relaxation for Valid Upper Bound 29

3.5 Experimental Results 31

3.6 Conclusion 33

4 Conclusion **35**

Bibliography **36**

Appendix Traffic Distributions for the RMSA Experiments **38**

List of Figures

Figure 2.1 Network Spain with five arbitrary requests. 5

Figure 2.2 Illustration of two configurations provisioning the requests in Fig. 2.1. 6

Figure 2.3 Higher-Level Column Generation. 10

Figure 2.4 Lower-Level Column Generation. 10

Figure 3.1 Flexible vs. Fixed Grid Optical Networks. 17

Figure 3.2 Spain network with five arbitrary requests. 21

Figure 3.3 Illustration of two configurations provisioning the requests in Fig. 3.2. 22

Figure 3.4 Nested column generation algorithm. 27

Figure 3.5 Illustration of the computed upper bound. 31

Figure A.1 Requests Distribution of RMSA Dataset SPAIN35-50. 38

Figure A.2 Requests Distribution of RMSA Dataset SPAIN45-60. 39

Figure A.3 Requests Distribution of RMSA Dataset SPAIN60-75. 39

Figure A.4 Requests Distribution of RMSA Dataset SPAIN64-85. 39

Figure A.5 Requests Distribution of RMSA Dataset SPAIN70-100. 40

Figure A.6 Requests Distribution of RMSA Dataset SPAIN80-120. 40

Figure A.7 Requests Distribution of RMSA Dataset SPAIN35-80. 40

Figure A.8 Requests Distribution of RMSA Dataset SPAIN45-110. 41

Figure A.9 Requests Distribution of RMSA Dataset SPAIN60-156. 41

Figure A.10 Requests Distribution of RMSA Dataset SPAIN64-170. 41

Figure A.11 Requests Distribution of RMSA Dataset SPAIN70-236. 42

Figure A.12 Requests Distribution of RMSA Dataset SPAIN80-256. 42

Figure A.13 Requests Distribution of RMSA Dataset SPAIN100-300. 42

Figure A.14 Requests Distribution of RMSA Dataset SPAIN120-300. 43
Figure A.15 Requests Distribution of RMSA Dataset SPAIN140-380A. 43
Figure A.16 Requests Distribution of RMSA Dataset SPAIN160-380A. 43
Figure A.17 Requests Distribution of RMSA Dataset SPAIN100-380. 44
Figure A.18 Requests Distribution of RMSA Dataset SPAIN120-380. 44
Figure A.19 Requests Distribution of RMSA Dataset SPAIN140-380B. 44
Figure A.20 Requests Distribution of RMSA Dataset SPAIN160-380B. 45
Figure A.21 Requests Distribution of RMSA Dataset USA100-380. 45
Figure A.22 Requests Distribution of RMSA Dataset USA120-380. 45
Figure A.23 Requests Distribution of RMSA Dataset USA140-380. 46
Figure A.24 Requests Distribution of RMSA Dataset USA160-380A. 46
Figure A.25 Requests Distribution of RMSA Dataset USA160-380B. 46
Figure A.26 Requests Distribution of RMSA Dataset USA180-380. 47
Figure A.27 Requests Distribution of RMSA Dataset USA200-380. 47
Figure A.28 Requests Distribution of RMSA Dataset USA220-380. 47
Figure A.29 Requests Distribution of RMSA Dataset USA276-380A. 48
Figure A.30 Requests Distribution of RMSA Dataset USA276-380B. 48
Figure A.31 Requests Distribution of RMSA Dataset USA276-380C. 48
Figure A.32 Requests Distribution of RMSA Dataset USA276-380D. 49
Figure A.33 Requests Distribution of RMSA Dataset USA276-380E. 49
Figure A.34 Requests Distribution of RMSA Dataset USA276-380F. 49
Figure A.35 Requests Distribution of RMSA Dataset USA524-380A. 50
Figure A.36 Requests Distribution of RMSA Dataset USA524-380B. 50
Figure A.37 Requests Distribution of RMSA Dataset USA524-380C. 50
Figure A.38 Requests Distribution of RMSA Dataset USA552-380. 51
Figure A.39 Requests Distribution of RMSA Dataset USA607-380A. 51
Figure A.40 Requests Distribution of RMSA Dataset USA607-380B. 51
Figure A.41 Requests Distribution of RMSA Dataset USA635-380. 52
Figure A.42 Requests Distribution of RMSA Dataset USA690-380. 52

List of Tables

Table 2.1 Comparison of RSA Experimental Results with Previous Studies . . . 13
Table 2.2 RSA Experimental Results of Larger Spain Datasets 14
Table 2.3 RSA Experimental Results of USA Datasets 14
Table 2.4 RSA Experimental Results of Larger USA Datasets 15
Table 3.1 Modulation data 31
Table 3.2 RMSA Experimental Results of Small-Medium Spain Datasets 32
Table 3.3 RMSA Experimental Results of Large Spain Datasets 32
Table 3.4 RMSA Experimental Results of Medium-Large USA Datasets 33
Table 3.5 RMSA Experimental Results of Larger USA Datasets 33

Chapter 1

Introduction

1.1 Background

With the rapidly growing demand in the optical networking sector, it has become more and more challenging to efficiently use the frequency spectrum already existing the optical layer. Research efforts to develop new technologies, that allow such efficient utilization, go hand in hand with the research efforts dedicated to develop efficient algorithms to solve the network planning problems based on these technologies.

One of these technologies is the Orthogonal Frequency Division Multiplexing (OFDM) [Saeki, 1999], which has given birth to the crucial network planning problems: the Routing and Spectrum Assignment (RSA) problem, and its extension, the Routing, Modulation and Spectrum Assignment (RMSA) problem.

1.2 Motivation

Our motivation in this research is to go one step further towards reducing the gap between the sizes of the RSA and RMSA problems that can be solved using the existing algorithms and the realistic problem sizes. In other words, to introduce decomposition models and develop exact algorithms capable of solving larger instances than what have been already solved in literature.

1.3 Contribution

In this research, we propose decomposition models for the RSA and RMSA problems based on lightpath configurations. As the proposed models have an exponential number of variables, we propose a nested column generation algorithm to efficiently solve each problem. Furthermore, we compute valid upper bounds using Lagrangian Relaxation in order to provide a measure of solution quality, which is the relative optimality gap.

Compared to the decompositions and algorithms in previous literature, the proposed decomposition and NCG algorithm efficiently produce higher-quality solutions. Furthermore, we were able to solve larger problem sizes than those already solved in literature.

1.4 Thesis Outline

In this thesis, the manuscripts of two publications are included. Chapter 2 is the manuscript of the first publication on solving the RSA problem, while Chapter 3 is the manuscript of the publication on solving the RMSA problem. Chapter 4 concludes the research presented in this thesis.

Chapter 2

Nested Column Generation Algorithm for the Routing and Spectrum Assignment Problem in Flexgrid Optical Networks

2.1 Introduction

The introduction of Orthogonal Frequency Division Multiplexing (OFDM) [Saeki, 1999] has opened the door to more efficient utilization of optical networks [Gerstel et al., 2012]. Yet, the same door has welcomed the new challenge of exploiting the full potential of such technology through the optimal provisioning of requested connections, known as the Routing and Spectrum Assignment (RSA) problem.

The outcome of the considerable research efforts put into developing algorithms for solving this problem can be classified into two main categories: heuristics and exact algorithms. Heuristics, e.g., [Christodoulopoulos et al., 2011, Alaskar et al., 2016], provide a fast solution, but this usually comes with no measure of solution quality. On the other hand, although early Integer Linear Programming (ILP) models, e.g., [Christodoulopoulos et al., 2010], were able to provide exact solutions, they had major scalability issues. This

has led to the exploration of decomposition models.

Ruiz et al. [2013] proposed an early decomposition model based on lightpaths. They developed a column generation algorithm as a solution scheme. Although they were able to efficiently solve small instances of the Spain network (21 nodes, 35 links) with 40 frequency slots and 64 requests, for larger instances of 96 slots and 180 requests, in the same network, the time limit of 10 hours was reached. Klinkowski et al. [2014] improved the formulation of Ruiz et al. [2013] with the use of valid inequalities. However, they could not go significantly beyond what was achieved in Ruiz et al. [2013].

Klinkowski et al. [2016] attempted to solve large instances using a branch-and-price algorithm, in which they used pre-computed paths. Hence, the proposed algorithm is not exact, and the optimal objective value of the Linear Programming (LP) relaxation is not a valid bound to asses the quality of the obtained ILP solution. Jaumard and Daryalal [2016] introduced a decomposition based on a subset of lightpaths having the same starting slot, called a lightpath configuration. They used two formulations for the pricing problem: one using pre-computed paths, and another link-formulation one to search thoroughly for the most improving configuration. However, the latter had scalability issues. More recently, Enoch and Jaumard [2018] improved the results of Jaumard and Daryalal [2016], with a shortest-path pricing problem and fine-tuning of the algorithm and its implementation, e.g., removing the columns with reduced cost coefficients less than a certain threshold, among other measures. They could reach higher-quality and more efficient solutions than in Jaumard and Daryalal [2016].

In this work, we use the same decomposition, based on a subset of lighpaths, as in Jaumard and Daryalal [2016], however with a different formulation. Furthermore, we propose a nested column generation algorithm to implicitly consider all possible lightpaths and all possible subsets of lightpaths.

2.2 Problem Statement

A flexible optical network can be represented by a directed graph $G = (V, L)$, with an optical node set V and a link set L. The bandwidth is sliced into a set of slots S. The

traffic is defined by a set of requests K, with every request having a source-destination node pair $(v_s, v_d)_k \in SD$ and a rate $r \in R$ represented by a number of slots, where SD is the set of source-destination node pairs, and R is the set of rates.

Given this network, the problem can be formally stated as finding, for every request, a routing path and a spectrum assignment such that the network throughput is maximum, while satisfying continuity and contiguity constraints. The continuity constraint requires that a request is assigned the same frequency slots along its entire path, while the contiguity constraint requires that the assigned frequency slots are contiguous, i.e., adjacent to each other, in the frequency domain.

2.3 Mathematical Model

We propose a decomposition scheme based on a lightpath configuration, which is a subset of requests having the same starting slot – hence, a configuration is indexed by $s \in S$. Figures 2.1 and 2.2 show illustrations of two different configurations starting at the slots s_i and s_j, respectively.

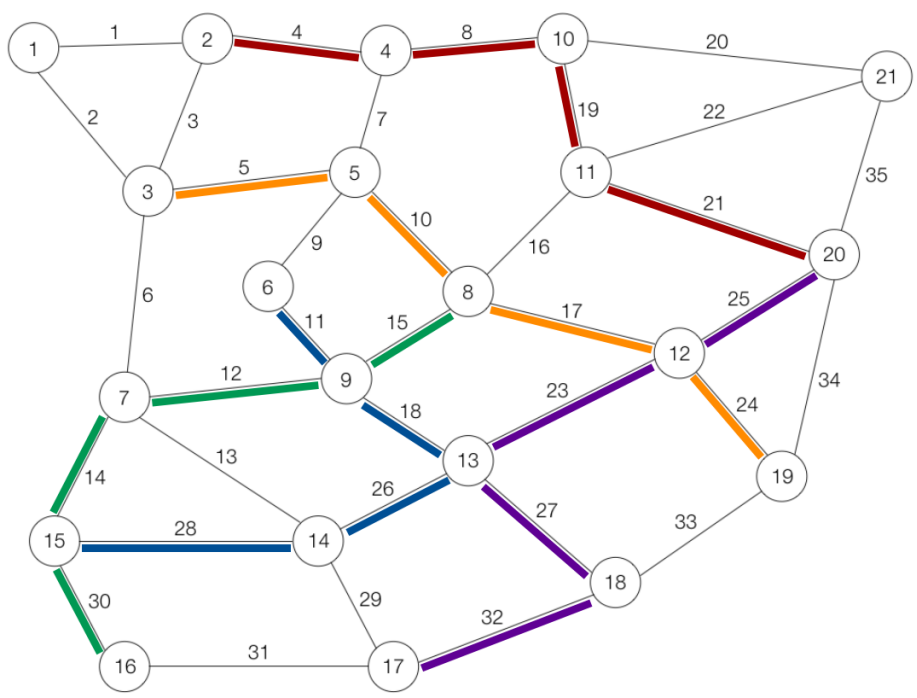

Figure 2.1: Network Spain with five arbitrary requests.

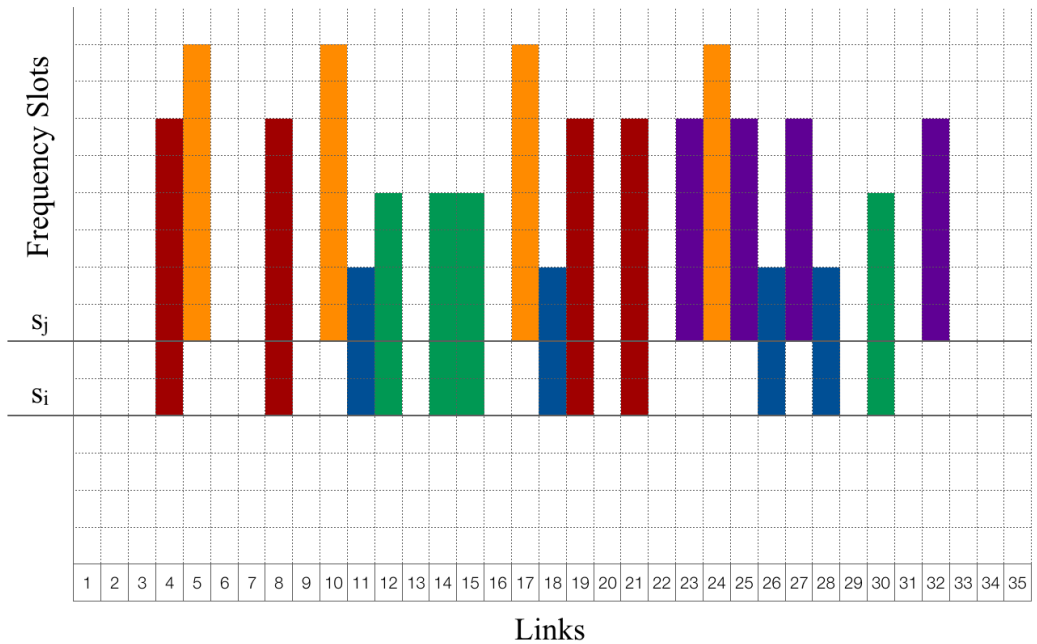

Figure 2.2: Illustration of two configurations provisioning the requests in Fig. 2.1.

2.3.1 Master Problem

Let K^r_{sd} be the set of requests with the source-destination node pair $(v_s, v_d) \in SD$ and rate $r \in R$, and $D^r_{sd} = |K^r_{sd}|$.

We introduce the decision variables: y^r_{sd}, which is the number of requests with the source-destination node pair $(v_s, v_d) \in SD$ and rate $r \in R$ that have been granted; and z_c, which is equal to 1 if the configuration $c \in C$ is granted, and to 0 otherwise.

The parameter a^c_k is equal to 1 if the configuration $c \in C$ contains the request $k \in K$, and to 0 otherwise; while the parameter δ^c_{sl} is equal to 1 if the slot $s \in S$ on the link $l \in L$ is occupied by the configuration $c \in C$, and to 0 otherwise.

The mathematical model of the master problem can then be written as follows:

$$\max \sum_{(v_s,v_d)\in SD} \sum_{r\in R} r\, y^r_{sd} \tag{1}$$

subject to:

$$\sum_{c \in C_s} z_c \leq 1 \qquad s \in S \tag{2}$$

$$y^r_{sd} \leq \sum_{c \in C} \sum_{k \in K^r_{sd}} a^c_k z_c \qquad (v_s, v_d) \in SD, r \in R \tag{3}$$

$$y^r_{sd} \leq D^r_{sd} \qquad (v_s, v_d) \in SD, r \in R \tag{4}$$

$$\sum_{c \in C} \delta^c_{sl} z_c \leq 1 \qquad s \in S, l \in L \tag{5}$$

$$z_c \in \{0, 1\} \qquad c \in C \tag{6}$$

$$y^r_{sd} \in \mathbb{Z}^+ \qquad (v_s, v_d) \in SD, r \in R. \tag{7}$$

By relaxing the integrality in the constraints (6) and (7), this problem can be solved using column generation with a pricing problem that generates, at every iteration, the most improving configuration for every starting slot $\sigma \in S$.

2.3.2 Higher-Level Pricing Problem

The Higher-Level Pricing Problem (HLPP) is the configuration generator, indexed by the starting slot $\sigma \in S$.

Let P_k be the set of routing paths for request $k \in K$. β^k_p is a decision variable that is equal to 1 if the path $p \in P_k$ is selected to route the request $k \in K$, and to 0 otherwise. The parameter δ^l_p is equal to 1 if the path $p \in P_k$ contains the link $l \in L$, and to 0 otherwise. We denote by $u^{(2)}_\sigma$, $u^{(3)}_{sd,r}$ and $u^{(5)}_{s'l}$ the values of the dual variables associated with the master problem's constraints (2), (3) and (5).

The mathematical model of the HLPP can be written as follows:

$$\max \quad -u^{(2)}_\sigma + \sum_{(v_s,v_d) \in SD} \sum_{r \in R} \sum_{k \in K^r_{sd}} \sum_{p \in P_k} \left(u^{(3)}_{sd,r} - \sum_{l \in L} \sum_{s'=\sigma}^{\sigma+r_k} u^{(5)}_{s'l} \delta^l_p \right) \beta^k_p \tag{8}$$

subject to:

$$\sum_{k \in K} \sum_{p \in P_k} \delta_p^l \beta_p^k \leq 1 \qquad l \in L \tag{9}$$

$$\sum_{p \in P_k} \beta_p^k \leq 1 \qquad k \in K \tag{10}$$

$$\beta_p^k \in \{0, 1\} \qquad p \in P_k, k \in K \tag{11}$$

The correspondence between the variables of the HLPP and the parameters of the master problem is as follows:

$$a_k = \sum_{p \in P_k} \beta_p^k \qquad k \in K \tag{12}$$

$$\delta_{s'l} = \sum_{k \in K : s' \in [\sigma, \sigma + r_k]} \sum_{p \in P_k} \delta_p^l \beta_p^k \qquad l \in L, s' \in S \tag{13}$$

By relaxing the integrality in the constraint (11), this problem can also be solved using column generation as a master problem to a lower-level pricing problem that will generate, at every iteration, the most improving routing path for every request $k \in K$.

2.3.3 Lower-Level Pricing Problem

The Lower-Level Pricing Problem (LLPP) is the path generator, indexed by the starting slot $\sigma \in S$ and the request $k \in K$.

Denoting by $u_l^{(9)}$ and $u_k^{(10)}$ the values of the dual variables associated with the HLPP's constraints (9) and (10), respectively, and introducing the decision variable δ_l, which is equal to 1 if the link $l \in L$ is selected as part of the path being generated, and to 0 otherwise, the mathematical model of the LLPP can be written as follows:

$$\min \quad \sum_{l \in L} \left(\sum_{s'=\sigma}^{\sigma + r_k} u_{s'l}^{(5)} + u_l^{(9)} \right) \delta_l - u_{sd,r}^{(3)} + u_k^{(10)} \tag{14}$$

subject to:

$$\sum_{l \in \delta^+(v_s)} \delta_l - \sum_{l \in \delta^-(v_s)} \delta_l = 1 \tag{15}$$

$$\sum_{l \in \delta^-(v_d)} \delta_l - \sum_{l \in \delta^+(v_d)} \delta_l = 1 \tag{16}$$

$$\sum_{l \in \delta^+(i)} \delta_l - \sum_{l \in \delta^-(i)} \delta_l = 0 \qquad i \in V \setminus \{v_s, v_d\} \tag{17}$$

$$\delta_l \in \{0, 1\} \qquad l \in L \tag{18}$$

This is a shortest path problem that can be solved exactly using an efficient algorithm, e.g., Dijkstra's algorithm.

2.4 Solution Scheme

2.4.1 Nested Column Generation

We propose a nested column generation algorithm which consists of two levels. In the Higher-Level Column Generation (HLCG), in Figure 2.3, the HLPP generates the configuration that will produce the largest improvement in the master problem's objective value. This level terminates when no more improving configurations can be generated.

At every iteration of the HLCG, the HLPP is solved through the Lower-Level Column Generation (LLCG), in Figure 2.4, in which the HLPP is the master problem to the LLPP which generates at every iteration the path that will produce the largest improvement in HLPP's objective value, and this level terminates when no improving paths can be generated.

2.4.2 Accuracy

Starting from the LLPP, this shortest path problem can be solved exactly using an exact algorithm, e.g., Dijkstra's algorithm. Therefore, when the LLCG terminates, the Linear Programming (LP) objective value of the HLPP is a valid upper bound on its Integer Linear Programming (ILP) optimal objective value, and hence the HLPP solution is an ϵ-optimal

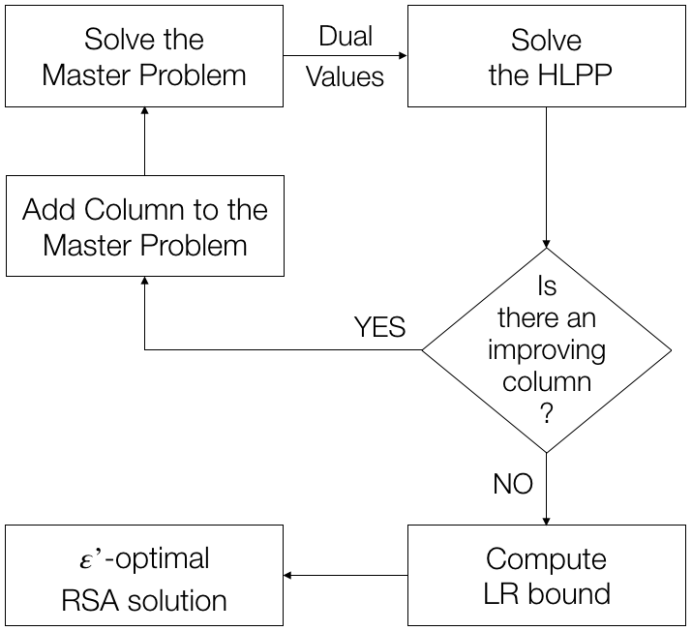

Figure 2.3: Higher-Level Column Generation.

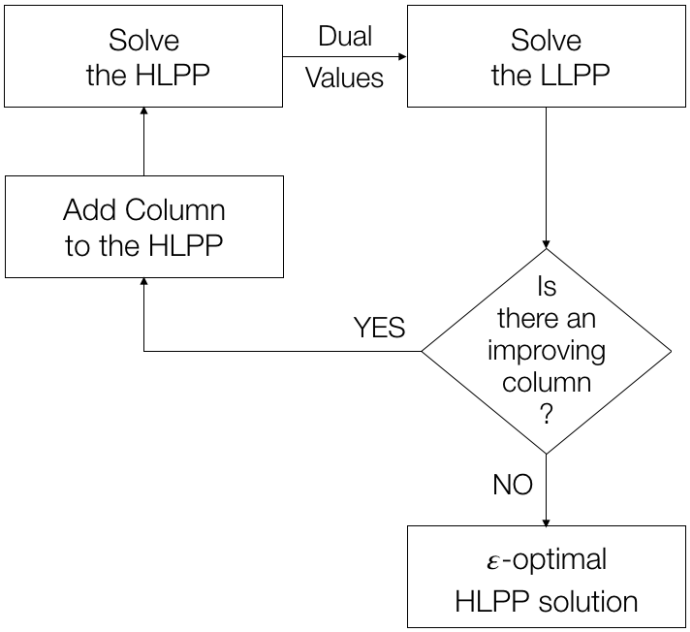

Figure 2.4: Lower-Level Column Generation.

solution. As for the HLCG, since the HLPP's solution is ϵ-optimal, the LP objective value of the master problem, upon the termination of the HLCG, is not a valid bound on its ILP optimal objective value. Consequently, to calculate the ϵ' relative optimality gap for the master problem, a valid upper bound has to be computed—we compute the Lagrangian Relaxation (LR) bound.

Following Vanderbeck and Wolsey [1995] and Pessoa et al. [2018], a valid upper-bound for the master problem can be computed at every iteration τ of the HLCG using Lagrangian Relaxation as follows:

$$L(u_\tau, x_{RC^\star})^{\text{MASTER}} = u_\tau^{\text{MASTER}}\, b + \text{RC}_{\text{ILP}}^{\star,\tau(\text{HLPP})} \leq \\ u_\tau^{\text{MASTER}}\, b + \text{RC}_{\text{LP}}^{\star,\tau(\text{HLPP})} = z_{\text{LR}}^{\tau} \geq z_{\text{LP}}^{\tau(\text{MASTER})} \quad (19)$$

Where $\text{RC}^\star$ is the reduced cost coefficient, u_τ^{MASTER} is the vector of the dual variables associated with the master problem's constraints at iteration τ of the HLCG, and b is the vector of the right-hand side of the master problem's constraints.

Since the LR bound is not monotonically improving [Pessoa et al., 2018], the best LR bound, i.e., the minimum throughout all the iterations, should be selected. Furthermore, since the LP optimal objective value can never exceed the offered load, this offered load is also a valid upper bound. Hence, the best possible upper bound should be computed as follows:

$$\overline{z}_{\text{LP}} = \min \{ \min_{\tau} z_{\text{LR}}^{\tau} \text{ , Offered Load } \} \quad (20)$$

2.5 Experimental Results

For the experimentation purposes, we solve four different groups of datasets. The first group is the same datasets solved by both Jaumard and Daryalal [2016] and Enoch and Jaumard [2018] for the network Spain (21 nodes, 35 links). Table 2.1 summarizes the comparison of these datasets' solutions. Although the solution quality of the proposed algorithm is

comparable to Enoch and Jaumard [2018] for this group of datasets, the running time is actually not. This is because the implementation of Enoch and Jaumard [2018] has much fine tuning, including fine tuning of the CPLEX parameters, which are not practical to fine tune for every problem instance.

In addition to the CPU time, we use the relative optimality gap (ϵ), defined in (21), and the Grade of Service (GoS), defined in (22), as comparison measures.

$$\epsilon = \frac{\overline{z}_{\text{LP}} - z_{\text{ILP}}}{z_{\text{ILP}}} \times 100\% \tag{21}$$

$$\text{GoS} = \frac{\text{Granted Bandwidth}}{\text{Requested Bandwidth}} = \frac{z_{\text{ILP}}}{\text{Offered Load}} \times 100\% \tag{22}$$

Table 2.1: Comparison of RSA Experimental Results with Previous Studies

Problem Instance			Current Study						Study of Jaumard and Daryalal [2016]					Study of Enoch and Jaumard [2018]				
Load (Tbps)	$\|K\|$	$\|S\|$	z_{LP}	z_{ILP}	z_{LR}	GoS (%)	ϵ' (%)	CPU (sec.)	z_{LP}	z_{ILP}	GoS (%)	ϵ (%)	CPU (sec.)	z_{LP}	z_{ILP}	GoS (%)	ϵ (%)	CPU (sec.)
3.7	35	50	3.7	3.7	4.0	100	0.0	2.9	3.7	3.2	86	16	50	3.7	3.7	100	0.0	0.3
4.8	45	60	4.8	4.8	5.1	100	0.0	3.6	4.8	4.2	88	14	86	4.8	4.8	100	0.0	0.4
6.8	60	75	6.8	6.8	7.9	100	0.0	6.0	6.8	5.8	85	18	147	6.8	6.8	100	0.0	0.7
7.5	64	85	7.5	7.5	8.5	100	0.0	7.4	7.5	6.0	80	24	176	7.5	7.5	100	0.0	1.3
7.4	70	100	7.4	7.4	8.2	100	0.0	9.2	7.4	6.2	84	20	263	7.4	7.4	100	0.0	1.7
9.7	80	120	9.7	9.7	10.8	100	0.0	14.0	9.7	8.2	85	19	323	9.7	9.7	100	0.0	2.5
7.5	35	80	7.5	7.5	8.6	100	0.0	6.9	7.5	6.7	89	11	134	7.5	7.5	100	0.0	0.9
9.8	45	110	9.8	9.8	11.3	100	0.0	12.1	9.8	8.8	90	11	177	9.8	9.8	100	0.0	2.0
10.7	60	156	10.7	10.7	11.3	100	0.0	25.4	10.7	9.5	89	13	261	10.7	10.7	100	0.0	3.1
15.5	64	170	15.5	15.5	16.2	100	0.0	40.6	15.5	13.0	84	20	630	15.5	15.5	100	0.0	4.7
15.1	70	236	15.1	15.1	16.2	100	0.0	53.5	15.1	13.1	87	15	1342	15.1	15.1	100	0.0	7.8
16.9	80	256	16.9	16.9	19.5	100	0.0	66.7	16.9	14.5	86	17	1419	16.9	16.9	100	0.0	10.3

The second group is of larger datasets for the Spain network, i.e., with larger offered load and larger number of slots. The results of this second group are summarized in Table 2.2.

Table 2.2: RSA Experimental Results of Larger Spain Datasets

Problem Instance			z_{LP}	z_{ILP}	z_{LR}	GoS (%)	ϵ' (%)	CPU (min.)
Load (Tbps)	$\lvert K\rvert$	$\lvert S\rvert$						
8.1	100	300	8.1	8.1	9.3	100	0.0	1.3
9.6	120	300	9.6	9.6	10.4	100	0.0	1.4
11.2	140	380	11.2	11.2	14.3	100	0.0	2.1
13.3	160	380	13.3	13.3	14.2	100	0.0	2.5
21.9	100	380	21.9	21.9	24.0	100	0.0	3.4
25.6	120	380	25.6	25.6	29.2	100	0.0	4.2
29.7	140	380	29.7	29.7	33.0	100	0.0	4.6
33.7	160	380	33.7	33.7	36.5	100	0.0	4.7

The third group of datasets is for the USA network (24 nodes, 86 links), and their results are summarized in Table 2.3.

Table 2.3: RSA Experimental Results of USA Datasets

Problem Instance			z_{LP}	z_{ILP}	z_{LR}	GoS (%)	ϵ' (%)	CPU (min.)
Load (Tbps)	$\lvert K\rvert$	$\lvert S\rvert$						
21.9	100	380	21.9	21.9	26.3	100	0.0	7.1
29.7	140	380	29.7	29.7	34.5	100	0.0	11.5
43.1	160	380	43.1	43.1	50.9	100	0.0	15.0
59.7	220	380	59.7	59.7	65.9	100	0.0	15.2
72.3	276	380	72.3	72.3	82.2	100	0.0	20.9
76.7	276	380	76.7	76.7	85.0	100	0.0	23.1
85.3	276	380	85.3	85.3	96.9	100	0.0	21.3
90.9	276	380	90.9	90.9	100.0	100	0.0	19.5

For the larger instances of Spain and USA networks, the proposed algorithm produces higher-quality solution than Enoch and Jaumard [2018] which had an average of 10% optimality gap and 90% GoS, compared to 0% and 100%, respectively, in our case for similarly-sized datasets.

The fourth group is of larger instances for the USA network, with offered load up to double that in Enoch and Jaumard [2018] and in our third group of datasets. As Table 2.4 shows, the results has high-quality solutions, i.e., small relative optimality gap; high GoS;

and reasonable efficiency, i.e., less than an hour for this planning problem.

Table 2.4: RSA Experimental Results of Larger USA Datasets

Problem Instance			z_{LP}	z_{ILP}	z_{LR}	GoS (%)	ϵ' (%)	CPU (min.)
Load (Tbps)	$\lvert K\rvert$	$\lvert S\rvert$						
143.8	524	380	139.0	139.0	173	97	3.5	31.8
145.0	524	380	139.3	139.3	143	96	2.6	31.3
146.3	524	380	141.2	141.1	145	96	2.6	58.2
151.9	552	380	142.6	142.6	157	94	6.5	32.6
160.6	607	380	149.4	149.4	151	93	0.7	31.8
161.4	607	380	153.4	153.4	164	95	5.2	34.4
168.7	635	380	157.7	157.7	168	93	6.6	34.5
179.6	690	380	161.5	161.0	178	90	10.8	36.0

2.6 Conclusion

In this paper we have proposed a formulation and a nested column generation algorithm to solve the Routing and Spectrum Assignment problem in flexible optical networks. Compared to recent studies, our algorithm produces high-quality solutions quite efficiently.

Chapter 3

Nested Column Generation for Large-Scale Routing, Modulation and Spectrum Assignment in Flexible Optical Networks

3.1 Introduction

The steadily growing demand in the optical networking sector is challenging both service providers and researchers to develop new technologies for efficient utilization of the frequency spectrum of the optical layer. However, the full potential of these new technologies would not be reached without developing efficient algorithms to solve the network planning problems based on these new technologies. In this paper, we consider the Orthogonal Frequency Division Multiplexing (OFDM) generation of optical networks and the crucial planning problem introduced by this technology: the Routing, Modulation and Spectrum Assignment problem.

3.1.1 Technical Background

The introduction of Orthogonal Frequency Division Multiplexing (OFDM) [Saeki, 1999] has opened the door to more efficient utilization of the frequency spectrum in optical fiber networks. Its modulation technique has enabled finer allocation of the optical spectrum with granularity smaller than wavelength [Gerstel et al., 2012], providing a flexible grid in contrast to a fixed grid. Figure 3.1 illustrates how efficiently the optical spectrum is used in the case of a flexible grid compared to a fixed grid.

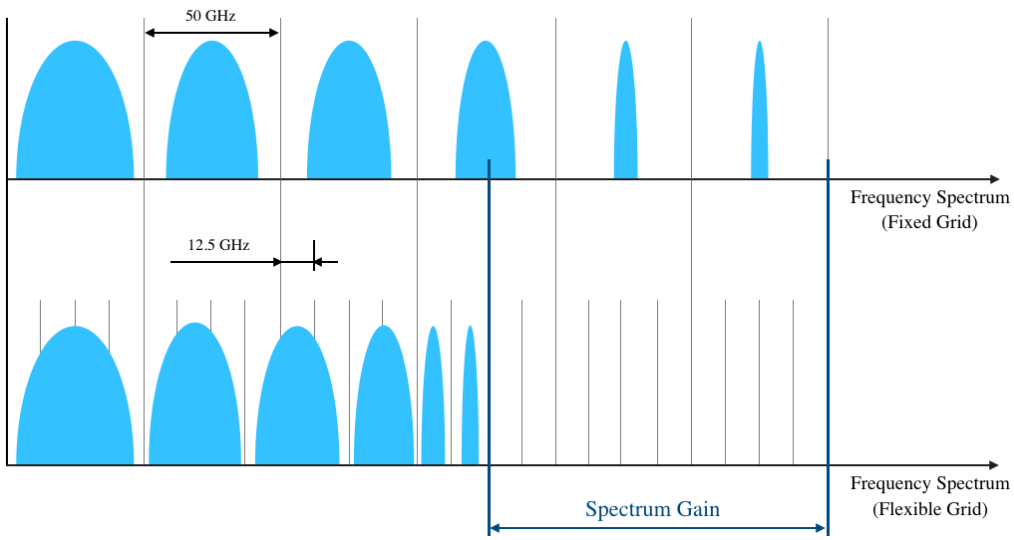

Figure 3.1: Flexible vs. Fixed Grid Optical Networks.

Although such technology allows more efficient utilization of the frequency spectrum, it made the problem of provisioning connection requests more challenging; giving birth to the Routing, Modulation and Spectrum Assignment (RMSA) problem.

3.1.2 Literature Review

The RMSA is one of the problems widely addressed in literature, with and without the modulation aspect – the variant without the modulation aspect is the Routing and Spectrum Assignment (RSA) problem. The algorithms proposed in the previous research are mostly either heuristics or exact algorithms, with machine learning techniques recently being explored.

Although heuristics, e.g., [Christodoulopoulos et al., 2011, Alaskar et al., 2016], provide efficient solutions, they usually come with no measure of solution quality, i.e., how far the obtained solution is from the optimal solution. An example of a recent machine learning-based method for the RMSA problem can be found in Chen et al. [2018], which uses reinforcement learning to solve dummy to small-sized networks. However, in this paper, we focus on exact algorithms and decomposition models.

While early Integer Linear Programming (ILP) models, e.g., [Christodoulopoulos et al., 2010], could provide exact solutions, they had major scalability issues. This has encouraged the investigation of decomposition models.

Ruiz et al. [2013] proposed a first lightpath-based decomposition model along with a column generation algorithm. For the Spain network (21 nodes, 35 links), they were able to solve small instances of 40 frequency slots and up to 64 requests in less than 30 seconds. However, for larger instances of up to 96 slots and 180 requests, the running time reached the limit of 10 hours. Klinkowski et al. [2014] improved the formulation of Ruiz et al. [2013] with the use of valid inequalities, but did not go significantly further than in Ruiz et al. [2013]. In an attempt to solve large instances, Klinkowski et al. [2016] proposed a Branch-and-Price algorithm. However, the resulting algorithm is not an exact algorithm and the optimal objective value of the Linear Programming (LP) relaxation is not a valid bound to assess the quality of the obtained ILP solutions. This is because the authors used pre-computed paths, and consequently did not consider, neither explicitly nor implicitly, all possible lightpaths. Jaumard and Daryalal [2016] proposed a decomposition based on a subset of lightpaths having the same starting slot, known as a lightpath configuration. They used two formulations for the pricing problem: one using pre-computed paths, and another link-formulation one to search thoroughly for the most improving configuration. However, the latter had scalability issues. More recently, Enoch and Jaumard [2018] improved the results of Jaumard and Daryalal [2016], with a shortest-path pricing problem and fine-tuning of the algorithm and its implementation, e.g., removing the columns with reduced cost coefficients less than a certain threshold, among other measures. They could reach higher-quality and more efficient solutions than in Jaumard and Daryalal [2016].

3.1.3 Contribution

In this paper, we employ the same decomposition as in Jaumard and Daryalal [2016], based on a light path configuration, but with a new formulation. The proposed model has an exponential number of lightpath configuration variables, therefore we propose a nested column generation algorithm to implicitly consider all possible lightpaths and all possible subsets of lightpaths. Furthermore, we use Lagrangian Relaxation to compute a valid upper bound on the ILP optimal objective value, in order to compute the relative optimality gap to assess the quality of the obtained solutions.

Compared to the decompositions and algorithms in the previous literature, the proposed decomposition and nestd column generation algorithm efficiently produce higher-quality solutions. Furthermore, we were able to solve larger problem sizes than those already solved in literature.

3.1.4 Paper Organization

In the next section, we formally define the RMSA problem. In section 3, we present the proposed decomposition model, which consists of a Master problem and two levels of sub-problems. In section 4, we propose the nested column generation algorithm and explain the computation of the valid upper bound using Lagrangian Relaxation. In section 5, we present the experimental results obtained using the proposed model and algorithm. And in the last section, we conclude the work presented in this paper.

3.2 Problem Statement

The topology of a flexible optical fiber network can be represented by a directed graph $G = (V, L)$, where V represents the set of optical nodes, and L represents the set of optical fiber links. The optical spectrum on each fiber link is sliced into a set S of frequency slots of equal width w. The network traffic is defined by the set of connection requests K, where every request $k \in K$ is characterized by the following: a source-destination node pair $(v_s, v_d)_k \in SD$, where $v_s^k \in V$ is the source node of request $k \in K$, $v_d^k \in V$ is the destination node of request $k \in K$, and SD is the set of source-destination node pairs; and a rate $r_k \in R$

in Giga bit per second (Gbps), where R is the set of rates. Furthermore, we have the set M of modulations where every modulation $m \in M$ is characterized by the following: a spectral efficiency c_m, and a maximum reach d_m, which is the maximum distance in kilometer that a request can be routed through using modulation $m \in M$.

According to the previous description, the RMSA problem can be formally defined as follows: finding for every request $k \in K$ a routing path, a modulation and a frequency assignment that would maximize the network throughput while respecting the continuity and contiguity constraints. A routing path is simply a subset of links leading from the source node $v_s^k \in V$ to the destination node $v_d^k \in V$. The spectrum assignment is the set of frequency slots assigned to the request $k \in K$, according to the selected modulation $m \in M$, with a total number of D_k. The network throughput is the total granted bandwidth, which is the total rate of all granted requests. The continuity constraint states that a request $k \in K$ is assigned the same frequency slots along it routing path, while the contiguity constraint requires that these assigned frequency slots are contiguous, i.e., adjacent to each other, in the frequency spectrum.

3.3 Mathematical Formulation

We propose a mathematical formulation that is a decomposition model with an exponential number of variables intuitively, i.e., we did not start from a compact formulation, that has a polynomial number of variables, and then applied Dantzig-Wolfe reformulation, see Dantzig and Wolfe [1960].

3.3.1 Lightpath Configuration-Based Decomposition

Our decomposition model is based on a lightpath configuration. A lightpath is defined as a combination of a routing path and a frequency spectrum assignment, so, e.g., two different requests having the same exact routing path but different frequency spectrum assignment are simply routed through two different lightpaths. We then define a lightpath configuration $c \in C$ as a set of lightpaths having the same starting slot $\sigma \in S$, where C is the set of lightpath configurations which is of exponential cardinality.

To further illustrate what a lightpath configuration is, Figure 3.2 shows an arbitrary five requests in the Spain network, which are then provisioned through two different lightpath configurations in Figure 3.3. We can see that the lightpath configuration of slot s_i is the set of lightpaths provisioning the red, blue and green requests, and that all of the three light paths start at the same starting slot s_i. The same applies to the other example of the starting slot s_j with the orange and violet requests.

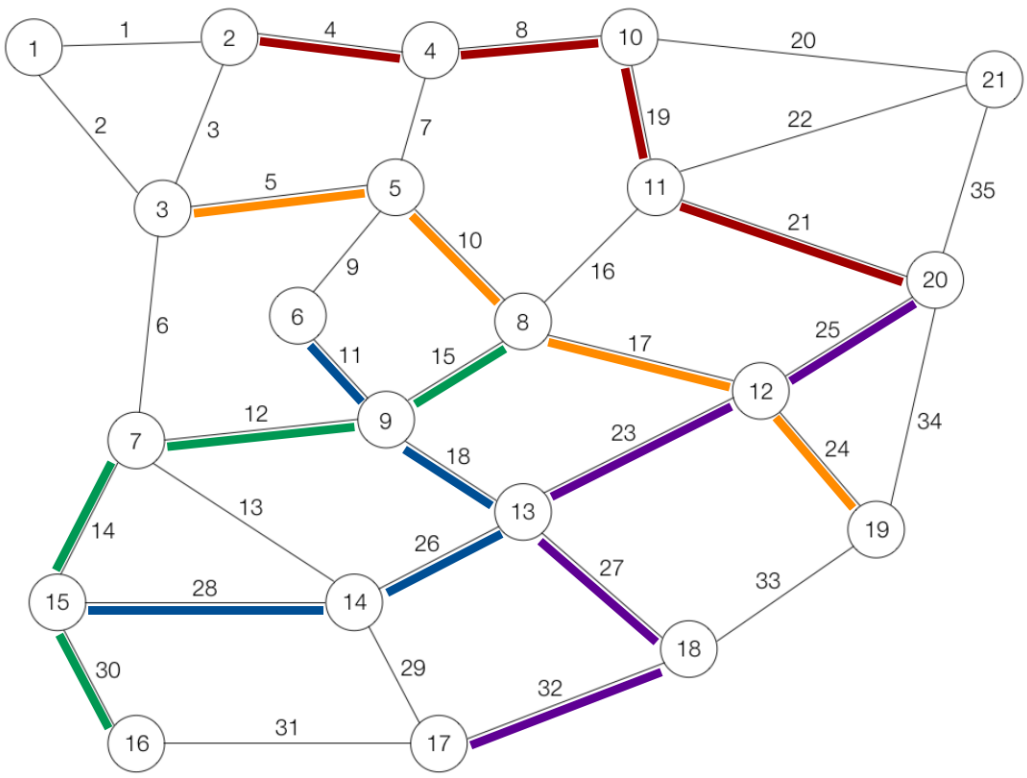

Figure 3.2: Spain network with five arbitrary requests.

3.3.2 Mater Problem

We introduce the following:

Sets and parameters:

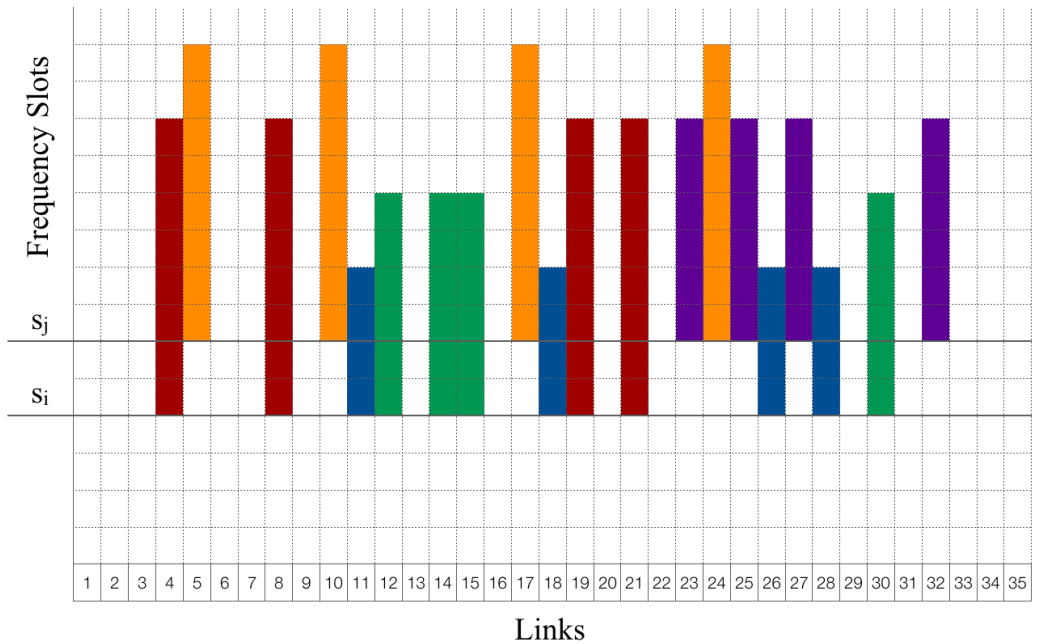

Figure 3.3: Illustration of two configurations provisioning the requests in Fig. 3.2.

K^r_{sd} The set of requests with the source-destination node pair $(v_s, v_d) \in SD$ and rate $r \in R$.

K^r_{sd} The number of requests with the source-destination node pair $(v_s, v_d) \in SD$ and rate $r \in R$.

a^c_k a parameter equal to 1 if the request $k \in K$ is provisioned through the lightpath configuration $c \in C$,

is equal to 0 otherwise.

δ^c_{sl} a parameter equal to 1 if the frequency slot $s \in S$ on the link $l \in L$ is occupied by the lightpath configuration $c \in C$,

is equal to 0 otherwise.

Decision variables:

y^r_{sd} The number of requests with the source-destination node pair $(v_s, v_d) \in SD$ and rate $r \in R$ that have been granted.

z_c a decision variable equal to 1 if the lightpath configuration $c \in C$ is granted,

is equal to 0 otherwise.

The mathematical model of the Master problem can then be written as follows:

$$\max \sum_{(v_s,v_d)\in SD} \sum_{r\in R} r\, y^r_{sd} \tag{23}$$

subject to:

$$\sum_{c\in C_s} z_c \leq 1 \qquad s \in S \tag{24}$$

$$y^r_{sd} \leq \sum_{c\in C} \sum_{k\in K^r_{sd}} a^c_k z_c \qquad (v_s, v_d) \in SD, r \in R \tag{25}$$

$$y^r_{sd} \leq D^r_{sd} \qquad (v_s, v_d) \in SD, r \in R \tag{26}$$

$$\sum_{c\in C} \delta^c_{sl} z_c \leq 1 \qquad s \in S, l \in L \tag{27}$$

$$z_c \in \{0, 1\} \qquad c \in C \tag{28}$$

$$y^r_{sd} \in \mathbb{Z}^+ \qquad (v_s, v_d) \in SD, r \in R. \tag{29}$$

The objective function (23) maximizes the total granted bandwidth. Constraint (24) makes sure that no more than one configuration is granted for the same starting slot. Constraint (25) implies that the granted bandwidth is bounded by the total bandwidth that can actually be granted. Constraint (26) ensures that no more bandwidth than what is requested is granted. Constraint (27) restricts the use of every frequency slot on every link to at most one configuration. Finally, constraints (28) and (29) define the domain of the decision variables z_c and y^r_{sd}, respectively.

By relaxing the integrality in the constraints (28) and (29), this problem can be solved iteratively using column generation, as it will be presented in the next section of the paper, with the Higher-Level Pricing Problem (HLPP) generating the best lightpath configuration at every iteration.

3.3.3 Higher-Level Pricing Problem

The HLPP is the configuration generator: it is indexed by the starting slot $\sigma \in S$ and it generates at every iteration, for every slot, the lightpath configuration that will produce the largest improvement in the objective value of the Master problem.

To formally define the HLPP, we introduce the following:

Sets and parameters:

P_k The set of routing paths for request $k \in K$.

δ_p^l a parameter equal to 1 if the path $p \in P_k$ contains the link $l \in L$, is equal to 0 otherwise.

$u_\sigma^{(24)}$ the value of the dual variable associated with the Master problem's constraint (24).

$u_{sd,r}^{(25)}$ the value of the dual variable associated with the Master problem's constraint (25).

$u_{s'l}^{(27)}$ the value of the dual variable associated with the Master problem's constraint (27).

Decision variable:

β_p^k a decision variable equal to 1 if the routing path $p \in P_k$ is selected for routing the request $k \in K$, is equal to 0 otherwise.

The mathematical model of the HLPP can then be written as follows:

$$\max \quad -u_\sigma^{(24)} + \sum_{(v_s,v_d)\in SD} \sum_{r\in R} \sum_{k\in K_{sd}^r} \sum_{p\in P_k} \left(u_{sd,r}^{(25)} - \sum_{l\in L} \sum_{s'=\sigma}^{\sigma+r_k} u_{s'l}^{(27)} \delta_p^l \right) \beta_p^k \tag{30}$$

subject to:

$$\sum_{k\in K} \sum_{p\in P_k} \delta_p^l \beta_p^k \leq 1 \qquad l \in L \tag{31}$$

$$\sum_{p\in P_k} \beta_p^k \leq 1 \qquad k \in K \tag{32}$$

$$\beta_p^k \in \{0,1\} \qquad p \in P_k, k \in K \tag{33}$$

The objective function (30) maximizes the reduced cost coefficient to generate the most

improving lightpath configuration. Constraint (31) ensures that all the selected routing paths, for all the requests, are disjoint. Constraint (32) limits the routing of every request to at most one routing path. Finally, constraint (33) defines the domain of the decision variable β_p^k.

By relaxing the integrality in the constraint (33), this problem can be solved iteratively using column generation by being a master problem to the Lower-Level Pricing Problem (LLPP) which will generate the most improving routing path for every request along with selecting a modulation for this request.

The parameters of the Master problem are related to the decision variables of the HLPP as follows:

$$a_k = \sum_{p \in P_k} \beta_p^k \qquad k \in K \tag{34}$$

$$\delta_{s'l} = \sum_{k \in K : s' \in [\sigma, \sigma + r_k]} \sum_{p \in P_k} \delta_p^l \beta_p^k \qquad l \in L, s' \in S \tag{35}$$

3.3.4 Lower-Level Pricing Problem

The LLPP is the path generator: it is indexed by the starting slot $\sigma \in S$ and the request $k \in K$, and it generates at every iteration the routing path for this request $k \in K$ that will produce the largest improvement in the objective value of the HLPP of the starting slot $\sigma \in S$. Furthermore, it selects the modulation used to provision the request $k \in K$.

To formally define the LLPP, we introduce the following:

Additional parameters:

$u_l^{(31)}$ the value of the dual variable associated with the HLPP's constraint (31).

$u_k^{(32)}$ the value of the dual variable associated with the HLPP's constraint (32).

Decision variable:

δ_l a decision variable equal to 1 if the link $l \in L$ is selected in the path being generated, is equal to 0 otherwise.

The mathematical model of the LLPP can then be written as follows:

$$\min \quad \sum_{l \in L} \left(\sum_{s'=\sigma}^{\sigma+D_k} u_{s'l}^{(27)} + u_l^{(31)} \right) \delta_l - u_{sd,r}^{(25)} + u_k^{(32)} \tag{36}$$

subject to:

$$\sum_{l \in \delta^+(v_s)} \delta_l - \sum_{l \in \delta^-(v_s)} \delta_l \; = \; 1 \tag{37}$$

$$\sum_{l \in \delta^-(v_d)} \delta_l - \sum_{l \in \delta^+(v_d)} \delta_l \; = \; 1 \tag{38}$$

$$\sum_{l \in \delta^+(i)} \delta_l - \sum_{l \in \delta^-(i)} \delta_l \; = \; 0 \qquad i \in V \setminus \{v_s, v_d\} \tag{39}$$

$$\delta_l \in \{0, 1\} \qquad l \in L \tag{40}$$

This is a shortest path problem, with the objective function (36) minimizing the weight of the path to generate the most improving one to the objective of the HLPP. Constraints (37) and (38) ensure that the path starts at the source node $v_s \in V$ and ends at the destination node $v_d \in V$, respectively. Constraint (39) implies the continuity of the path. Finally, constraint (40) defines the domain of the decision variable δ_l.

For every request, the selected modulation is the one that will produce the minimum-weight path using the minimum number of slots while respecting the modulation maximum reach. This is obtained by solving the LLPP as a shortest-path problem with resource constraints. Given the rate r_k of request $k \in K$, the spectral efficiency c_m of modulation $m \in M$, and the width w of the frequency slots, the number of slots D_k for every request $k \in K$ and every modulation $m \in M$ can be computed as follows:

$$D_k = \left\lceil \frac{\left(\frac{r_k}{c_m}\right)}{w} \right\rceil \tag{41}$$

3.4 Nested Column Generation

To solve the RMSA with the proposed decomposition model, we use column generation, introduced in Dantzig and Wolfe [1960], but with a nested structure: nested column

generation. The proposed nested column generation algorithm has two levels, which we call the Higher-Level Column Generation (HLCG) and the Lower-Level Column Generation (LLCG). The HLCG consists of the LP relaxation of the Master problem and the HLPP as its column generator, while the LLCG consists of the LP relaxation HLPP as a master problem to its column generator, which is the LLPP. The proposed nested column algorithm is illustarted in Figure 3.4, and is further explained in the following subsections.

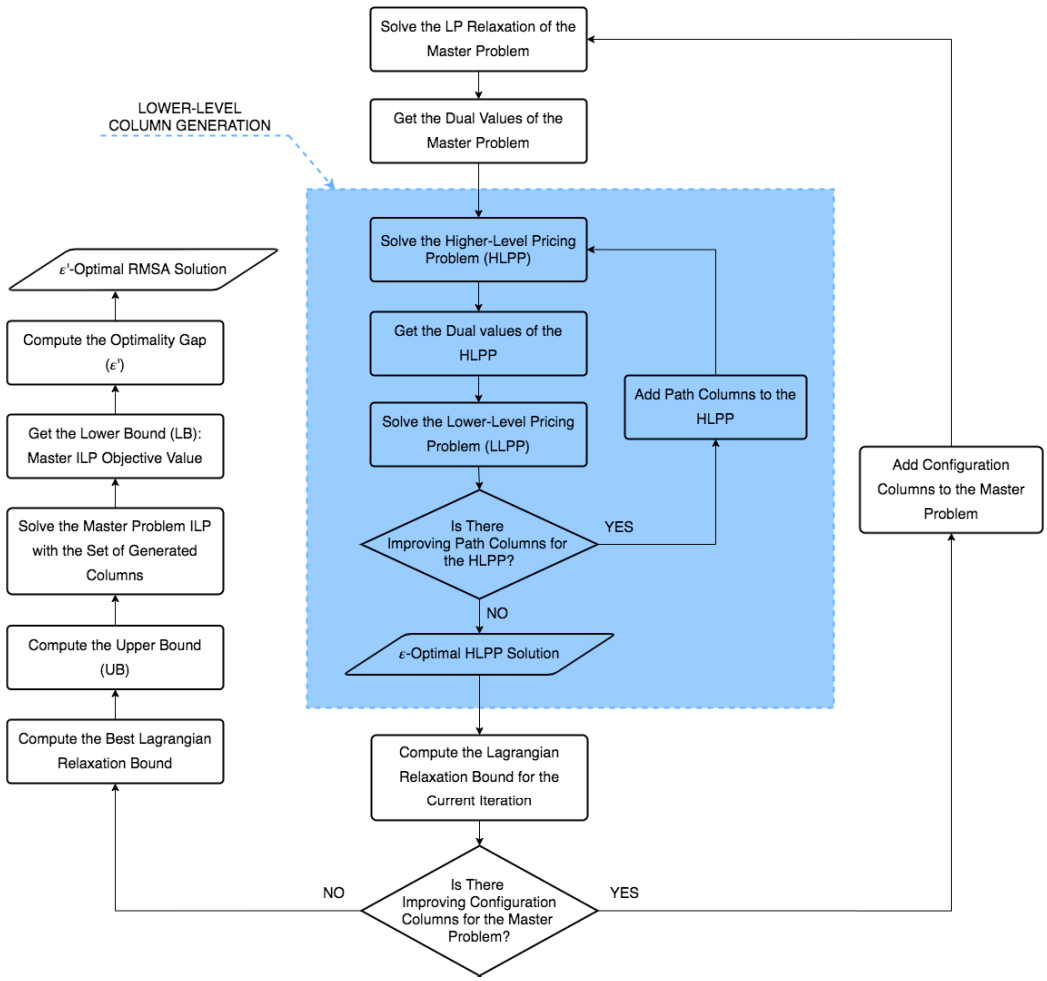

Figure 3.4: Nested column generation algorithm.

3.4.1 Higher-Level Column Generation

In the HLCG, the Master problem selects the lightpath configurations to be granted in order to maximize the granted bandwidth while respecting the previously discussed constraints. This problem is solved iteratively with the HLPP generating at every iteration a lightpath

configuration, for every starting slot, that will produce the largest improvement in the Master problem objective value. In other words, at every iteration, a set of lightpath configurations are generated, one for every starting slot, that will result in the maximum increase in the granted bandwidth. The iterations of the HLCG keep running as long as there still exists at least one improving lightpath configuration, which is determined by the reduced cost coefficient, i.e., the HLPP objective value. This HLCG terminates when no more improving columns can be generated, and then the Master problem ILP is solved with the set of generated configuration columns.

3.4.2 Lower-Level Column Generation

In the LLCG, the HLPP (indexed by the starting slot $\sigma \in S$) selects one path for every request that will produce the largest improvement in the HLPP objective value, i.e., the reduced cost coefficient, so that the HLPP can then produce the most improving lightpath configuration to the Master problem. Similar to the HLCG, the LLCG is solved iteratively, with the LLPP (indexed by the request $k \in K$ and the starting slot of its corresponding HLPP, $\sigma \in S$) generating at every iteration one routing path column to be added to the HLPP. The LLCG keeps iterating as long as there still exists at least one improving path column to be added to the HLPP. The LLCG terminates when no more improving path columns can be generated, and then the HLPP ILP is solved with the set of generated path columns. A full LLCG, for every starting slot $\sigma \in S$, runs until termination in every iteration of the HLCG.

3.4.3 Accuracy

To evaluate the accuracy of the proposed algorithm, we start from the lowest level and move upwards. The LLPP is a shortest path problem, which is solved exactly. Hence, the LP objective value of the HLPP is a valid upper bound on its ILP optimal objective value. Therefore, the obtained ILP solution for the HLPP is an ϵ-optimal solution, where ϵ is the relative optimality gap, calculated as follows:

$$\epsilon = \frac{\overline{z}_{\text{LP}} - z_{\text{ILP}}}{z_{\text{ILP}}} \times 100\% \tag{42}$$

In the HLCG, for the LP objective value of the master problem to be a valid upper bound on its ILP optimal objective value, the HLPP has to be solved exactly, i.e., using a branch-and-price algorithm, which is not the case, but rather an ϵ-optimal ILP solution is obtained. Consequently, the LP objective value of the master is not a valid upper bound on its ILP optimal objective value. This leads to the need of computing a valid upper bound on the ILP optimal objective value of the Master problem in order to compute its relative optimality gap, ϵ'. We therefore use Lagrangian Relaxation [Fisher, 1981] to compute this valid upper bound.

3.4.4 Lagrangian Relaxation for Valid Upper Bound

Following Vanderbeck and Wolsey [1995] and Pessoa et al. [2018], Lagrangian Relaxation can be used to obtain a valid upper bound on the optimal ILP objective value of the master problem, at any iteration of the column generation algorithm, by using the values of the dual variables of the master problem as the Lagrangian multipliers in the Lagrangian function. Introducing the following notation:

u^M	the vector of the dual variables values of the Master problem.
b^M	the vector of the constraints right-hand side of the Master problem.
c^M	the vector of the objective function coefficients of the Master problem.
A^M	the constraints coefficients matrix of the Master problem.
RC^{HLPP}	the reduced cost coefficient, i.e., the objective value of the HLPP

The Lagrangian function of the Master problem can then be written as follows:

$$\text{LR}(u^M, x) = \max_{x \in X} \left\{ L(u^M, x) = u^M b^M + \underbrace{(c^M - u^M A^M)x}_{\text{RC}^{\text{HLPP}}(u^M, x)} \right\} \tag{43}$$

At every iteration τ of the HLCG:

$$x_{\mathrm{RC}^\star} = \arg\max_{x \in X} L(u_\tau, x) \quad = \arg\max_{x \in X} \mathrm{RC}(u_\tau, x) \tag{44}$$

$$= \arg\max_{i \in I} \mathrm{RC}(u_\tau, x^i) = \arg \max_{x \in X^{\mathrm{HLPP}}} \mathrm{RC}^\star(u_\tau, x), \tag{45}$$

where $x^i, i \in I$ denote the extreme points of X, see Nemhauser and Wolsey [1988], Section II.3.6.

In the HLPP, $x_{\mathrm{RC}^\star}$ is known since we solve the LLPP exactly. Indeed $\mathrm{RC}_{\mathrm{ILP}}^{\star,\tau(\mathrm{HLPP})} \leq \mathrm{RC}_{\mathrm{LP}}^{\star,\tau(\mathrm{HLPP})}$, where $\mathrm{RC}_{\mathrm{ILP}}^{\star,\tau(\mathrm{HLPP})}$ and $\mathrm{RC}_{\mathrm{LP}}^{\star,\tau(\mathrm{HLPP})}$ are the optimal objective values of the ILP and the LP relaxation of the HLPP, respectively, at iteration τ of the HLCG. Consequently:

$$L(u_\tau, x_{\mathrm{RC}^\star})^{\mathrm{MASTER}} = u_\tau^M\, b + \mathrm{RC}_{\mathrm{ILP}}^{\star,\tau(\mathrm{HLPP})} \leq u_\tau^M\, b + \mathrm{RC}_{\mathrm{LP}}^{\star,\tau(\mathrm{HLPP})} = z_{\mathrm{LR}}^\tau > z_{\mathrm{LP}}^{\tau(\mathrm{MASTER})} \tag{46}$$

Since the Lagrangian Relaxation bound is not monotonically improving [Pessoa et al., 2018], the best LR bound, i.e., the minimum throughout all the iterations, should be selected as follows:

$$z_{\mathrm{LR}} = \min_\tau z_{\mathrm{LR}}^\tau \tag{47}$$

Since the total granted bandwidth cannot exceed the total requested bandwidth, i.e., the Offered Load, then the Offered Load is also a valid upper bound on the ILP optimal objective value of the Master problem. Therefore, the best upper bound should be computed as follows:

$$\overline{z}_{\mathrm{LP}} = \min \{\, z_{\mathrm{LR}} \;,\; \text{Offered Load} \,\} \tag{48}$$

Figure 3.5 shows the relative positions of the discussed values. We use tilde for feasible values, the star for optimal values and the overline for an upper bound. Regardless of the positions of the unknown ILP and LP optimal objectives values, the LP optimal objective

value is always an upper bound to the ILP optimal objective value, and the computed upper bound in (48) is always an upper bound to the LP optimal objective value, and hence, to the ILP optimal objective value.

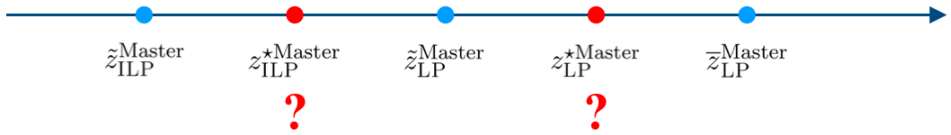

Figure 3.5: Illustration of the computed upper bound.

3.5 Experimental Results

In our experimentation, we considered four modulations: BPSK, QPSK, 8QAM and 16QAM. Table 3.1 summarizes the spectral efficiency as well as the maximum reach of these modulations, based on Huawei [2016].

Table 3.1: Modulation data

Modulation	Spectral efficiency (bit/sec/Hz)	Maximum reach (km)
BPSK	2	more than 4,000
QPSK	4	1,200 – 4,000
8QAM	6	600 – 1,200
16QAM	8	less than 600

We have experimented with different groups of datasets, starting with datasets for the Spain network (21 nodes, 35 links) similar in size and requests distribution to those solved in Jaumard and Daryalal [2016] and Enoch and Jaumard [2018], but of course, we consider the modulation aspect as well, while it was not considered in those two publications. Table 3.2 summarizes the results of these datasets.

We also compute the Grade of Service (GoS), which is defined as the ratio of the granted bandwidth to the total requested bandwidth, so the GoS can be calculated as follows:

$$\text{GoS} = \frac{z_{\text{ILP}}}{\text{Offered Load}} \times 100\% \tag{49}$$

Table 3.2: RMSA Experimental Results of Small-Medium Spain Datasets

Problem Instance				z_{LP} (Tbps)	z_{ILP} (Tbps)	z_{LR} (Tbps)	GoS (%)	ϵ' (%)	CPU (min.)
Name	Offered Load (Tbps)	$\|K\|$	$\|S\|$						
SPAIN35-50	3.7	35	50	3.7	3.7	3.7	100	0.0	0.06
SPAIN45-60	4.8	45	60	4.8	4.8	4.8	100	0.0	0.11
SPAIN60-75	6.8	60	75	6.8	6.8	7.2	100	0.0	0.2
SPAIN64-85	7.5	64	85	7.5	7.5	8.7	100	0.0	0.28
SPAIN70-100	7.4	70	100	7.4	7.4	7.7	100	0.0	0.29
SPAIN80-120	9.7	80	120	9.7	9.7	10.8	100	0.0	0.54
SPAIN35-80	7.5	35	80	7.5	7.5	7.7	100	0.0	0.27
SPAIN45-110	9.8	45	110	9.8	9.8	11.5	100	0.0	0.31
SPAIN60-156	10.7	60	156	10.7	10.7	14.3	100	0.0	0.58
SPAIN64-170	15.5	64	170	15.5	15.5	17.3	100	0.0	0.6
SPAIN70-236	15.1	70	236	15.1	15.1	16.0	100	0.0	1.22
SPAIN80-256	16.9	80	256	16.9	16.9	21.0	100	0.0	1.73

The second group of datasets is also for the Spain network but with larger offered load, larger number of requests and larger number of slots. Their results are summarized in Table 3.3.

Table 3.3: RMSA Experimental Results of Large Spain Datasets

Problem Instance				z_{LP} (Tbps)	z_{ILP} (Tbps)	z_{LR} (Tbps)	GoS (%)	ϵ' (%)	CPU (min.)
Name	Offered Load (Tbps)	$\|K\|$	$\|S\|$						
SPAIN100-300	8.1	100	300	8.1	8.1	9.7	100	0.0	2.37
SPAIN120-300	9.6	120	300	9.6	9.6	10.9	100	0.0	2.9
SPAIN140-380A	11.2	140	380	11.2	11.2	12.5	100	0.0	4.17
SPAIN160-380A	13.3	160	380	13.3	13.3	15.1	100	0.0	4.99
SPAIN100-380	21.9	100	380	21.9	21.9	23.0	100	0.0	4.45
SPAIN120-380	25.6	120	380	25.6	25.6	29.3	100	0.0	3.54
SPAIN140-380B	29.7	140	380	29.7	29.7	33.0	100	0.0	4.47
SPAIN160-380B	33.7	160	380	33.7	33.7	36.5	100	0.0	3.82

The third group of datasets is for the USA network (24 nodes, 86 links), with medium to large offered loads, numbers of requests and numbers of slots. In this group, we could solve instances as large as Enoch and Jaumard [2018], with quite higher solution quality and GoS. The results of these datasets are summarized in Table 3.4.

The last group is of larger instances for the USA network, with offered load up to double that in Enoch and Jaumard [2018]. As Table 3.5 shows, the obtained solutions are

Table 3.4: RMSA Experimental Results of Medium-Large USA Datasets

Problem Instance				z_{LP} (Tbps)	z_{ILP} (Tbps)	z_{LR} (Tbps)	GoS (%)	ϵ' (%)	CPU (min.)
Name	Offered Load (Tbps)	$\|K\|$	$\|S\|$						
USA100-380	21.9	100	380	21.9	21.9	26.4	100	0.0	6.68
USA120-380	25.6	120	380	25.6	25.6	29.1	100	0.0	8.13
USA140-380	29.7	140	380	29.7	29.7	37.7	100	0.0	11.7
USA160-380A	33.7	160	380	33.7	33.7	39.2	100	0.0	9.09
USA160-380B	43.1	160	380	43.1	43.1	51.0	100	0.0	10.84
USA180-380	49.3	180	380	49.3	49.3	54.4	100	0.0	11.25
USA200-380	54.7	200	380	54.7	54.7	60.4	100	0.0	12.25
USA220-380	59.7	220	380	59.7	59.7	74.4	100	0.0	14.93
USA276-380A	63.8	276	380	63.8	63.8	64.6	100	0.0	19.8
USA276-380B	61.0	276	380	61.0	61.0	69.6	100	0.0	12.87
USA276-380C	72.3	276	380	72.3	72.3	82.2	100	0.0	15.32
USA276-380D	76.7	276	380	76.7	76.7	77.6	100	0.0	23.4
USA276-380E	85.3	276	380	85.3	85.3	97.1	100	0.0	15.68
USA276-380F	90.9	276	380	90.9	90.9	100.1	100	0.0	14.55

of high quality, i.e., small relative optimality gap, and also with reasonable efficiency, as the maximum recorded running time is 41 minutes.

Table 3.5: RMSA Experimental Results of Larger USA Datasets

Problem Instance				z_{LP} (Tbps)	z_{ILP} (Tbps)	z_{LR} (Tbps)	GoS (%)	ϵ' (%)	CPU (min.)
Name	Offered Load (Tbps)	$\|K\|$	$\|S\|$						
USA524-380A	143.8	524	380	139.3	139.0	139.6	96.7	0.4	31.21
USA524-380B	145.0	524	380	140.3	139.9	150.3	96.5	3.6	31.52
USA524-380C	146.3	524	380	142.3	141.5	144.4	96.7	2.1	30.66
USA552-380	151.9	552	380	143.7	143.0	150.4	94.1	5.2	31.94
USA607-380A	160.6	607	380	150.6	149.9	157.7	93.3	5.2	35.05
USA607-380B	161.4	607	380	154.6	153.8	157.0	95.3	2.1	41.01
USA635-380	168.7	635	380	158.8	157.9	173.9	93.6	6.8	33.71
USA690-380	179.6	690	380	163.2	162.0	166.7	90.2	2.9	37.5

3.6 Conclusion

In this paper we proposed a decomposition model for the Routing, Modulation and Spectrum Assignment problem based on lightpath configurations. We have also proposed a nested column generation algorithm as a solution scheme. Furthermore, we used Lagrangian Relaxation to compute a valid upper bound on the optimal ILP objective value, and hence

compute the relative optimality gap as a measure of solution quality.

The obtained solutions, compared to those in the literature, are of higher quality and comparable efficiency. We were also able to solve data instances up to double the size of what has been already published.

Chapter 4

Conclusion

In this thesis, we proposed decomposition models for the RSA and RMSA problems based on lightpath configurations. As the proposed models have an exponential number of variables, we proposed a nested column generation algorithm to efficiently solve each problem. Furthermore, we compute valid upper bounds using Lagrangian Relaxation in order to provide a measure of solution quality, which is the relative optimality gap.

Compared to the decompositions and algorithms in previous literature, the proposed decomposition and nested column generation algorithm efficiently produce higher-quality solutions. Furthermore, we were able to solve larger problem sizes than those already solved in literature.

Bibliography

R.W. Alaskar, I. Ahmad, and A. Alyatama. Offline routing and spectrum allocation algorithms for elastic optical networks. *Optical Switching and Networking*, 21:79–92, 2016.

Xiaoliang Chen, Jiannan Guo, Zuqing Zhu, Roberto Proietti, Alberto Castro, and SJ Ben Yoo. Deep-rmsa: A deep-reinforcement-learning routing, modulation and spectrum assignment agent for elastic optical networks. In *2018 Optical Fiber Communications Conference and Exposition (OFC)*, pages 1–3. IEEE, 2018.

K. Christodoulopoulos, I. Tomkos, and E. A. Varvarigos. Routing and spectrum allocation in OFDM-based optical networks with elastic bandwidth allocation. In *IEEE Global Telecommunications Conference - GLOBECOM*, pages 1–6, 2010.

K. Christodoulopoulos, I. Tomkos, and E. Varvarigos. Elastic bandwidth allocation in flexible OFDM-based optical networks. *Journal of Lightwave Technology*, 29(9):1354 – 1366, May 2011.

George B Dantzig and Philip Wolfe. Decomposition principle for linear programs. *Operations research*, 8(1):101–111, 1960.

J. Enoch and B. Jaumard. Towards optimal and scalable solution for routing and spectrum allocation. *Electronic Notes in Discrete Mathematics (ENDM)*, 64C:335–344, 2018.

Marshall L Fisher. The lagrangian relaxation method for solving integer programming problems. *Management science*, 27(1):1–18, 1981.

O. Gerstel, M. Jinno, A. Lord, and S.J. Ben Yoo. Elastic optical networking: A new dawn for the optical layer? *IEEE Journal of Communications Magazine*, pages 512–520, February 2012.

Huawei. White paper on technological developments of optical networks. *Huawei Technologies Co., Ltd.*, 2016.

B. Jaumard and M. Daryalal. Scalable elastic optical path networking models. In *International Conference on Transparent Optical Networks - ICTON*, pages 1–4, 2016.

M. Klinkowski, M. Pioro, M. Zotkiewicz, M. Ruiz, and L. Velasco. Valid inequalities for the routing and spectrum allocation problem in elastic optical networks. In *International Conference on Transparent Optical Networks - ICTON*, pages 1–5, 2014.

M. Klinkowski, M. Zotkiewicz, K. Walkowiak, M. Pioro, M. Ruiz, and L. Velasco. Solving large instances of the rsa problem in flexgrid elastic optical networks. *IEEE/OSA Journal of Optical Communications and Networking*, 8:320 – 330, February 2016.

George L. Nemhauser and Laurence A. Wolsey. *Integer and Combinatorial Optimization*. Wiley, New York, 1988.

A. Pessoa, R. Sadykov, E. Uchoa, and F. Vanderbeck. Automation and combination of linear-programming based stabilization techniques in column generation. *INFORMS Journal on Computing*, 30(2):339–360, May 2018.

M. Ruiz, M. Zotkiewicz, L. Velasco, and J. Comellas. A column generation approach for large-scale RSA-based network planning. In *International Conference on Transparent Optical Networks - ICTON*, pages 53–64, 2013.

Tomoki Saeki. Orthogonal frequency division multiplexing, September 21 1999. US Patent 5,956,318.

F. Vanderbeck and L. A. Wolsey. An exact algorithm for ip column generation. *Operations Research Letters*, 19:151–159, 1995.

Appendix

Traffic Distributions for the RMSA Experiments

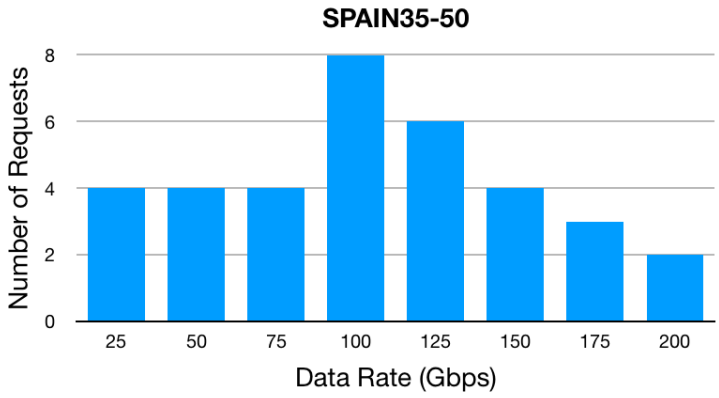

Figure A.1: Requests Distribution of RMSA Dataset SPAIN35-50.

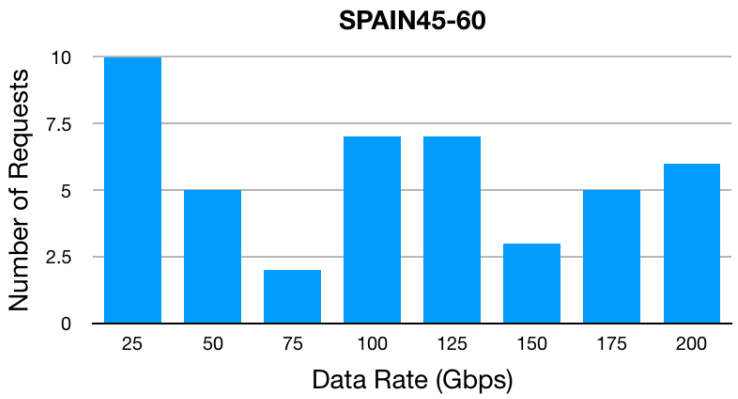

Figure A.2: Requests Distribution of RMSA Dataset SPAIN45-60.

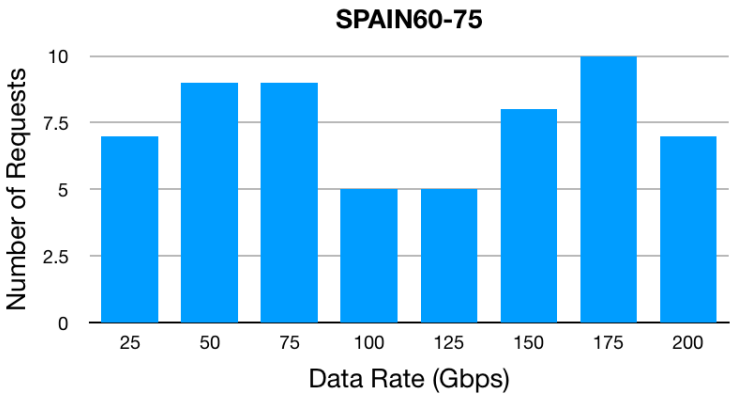

Figure A.3: Requests Distribution of RMSA Dataset SPAIN60-75.

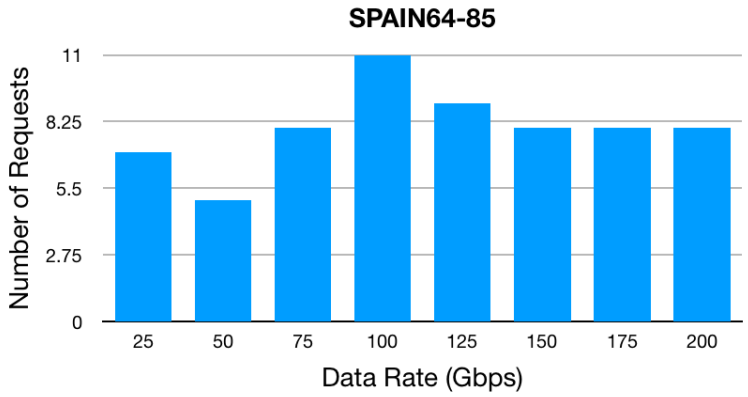

Figure A.4: Requests Distribution of RMSA Dataset SPAIN64-85.

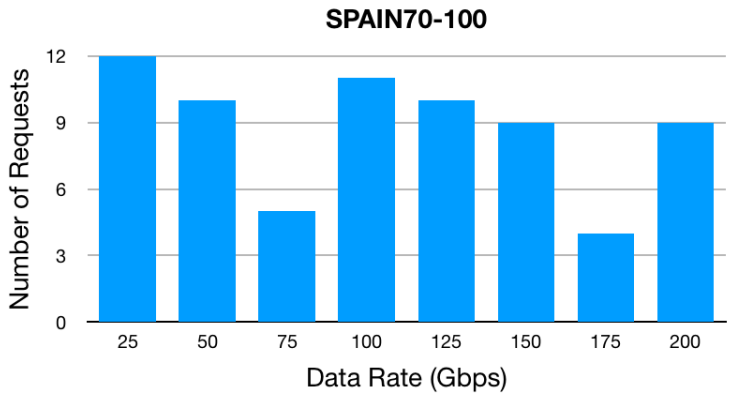

Figure A.5: Requests Distribution of RMSA Dataset SPAIN70-100.

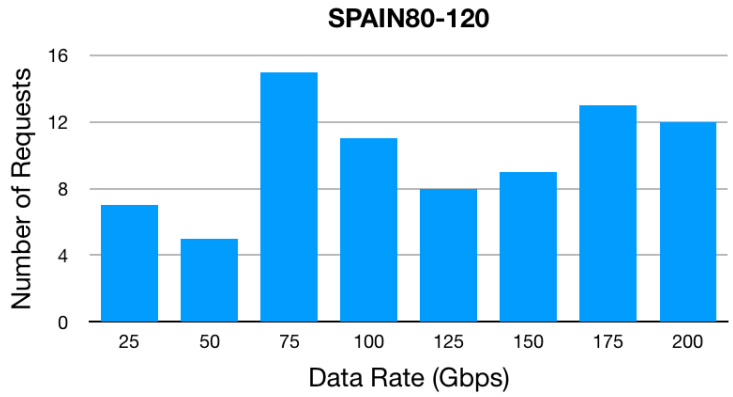

Figure A.6: Requests Distribution of RMSA Dataset SPAIN80-120.

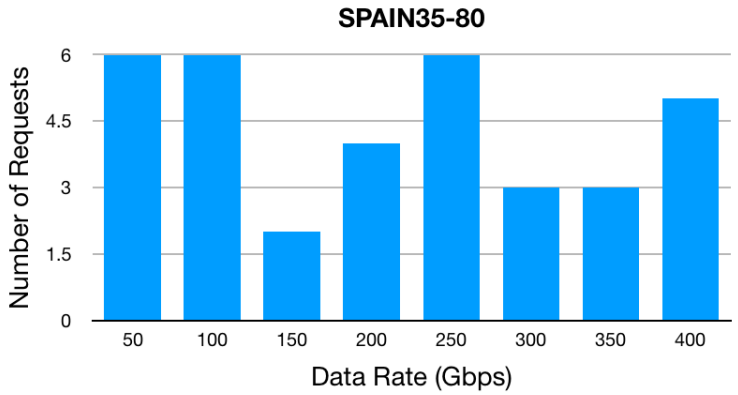

Figure A.7: Requests Distribution of RMSA Dataset SPAIN35-80.

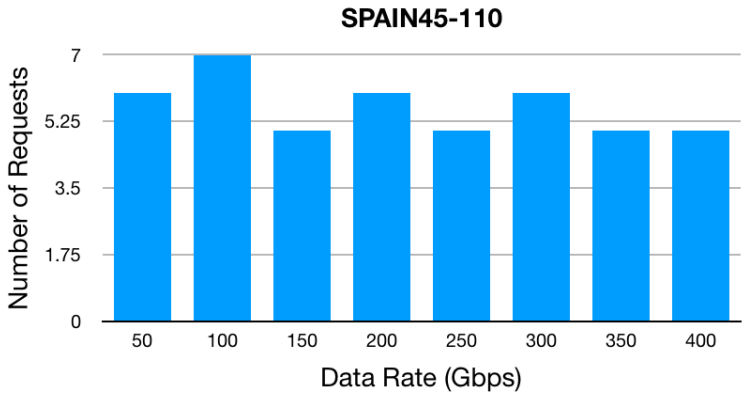

Figure A.8: Requests Distribution of RMSA Dataset SPAIN45-110.

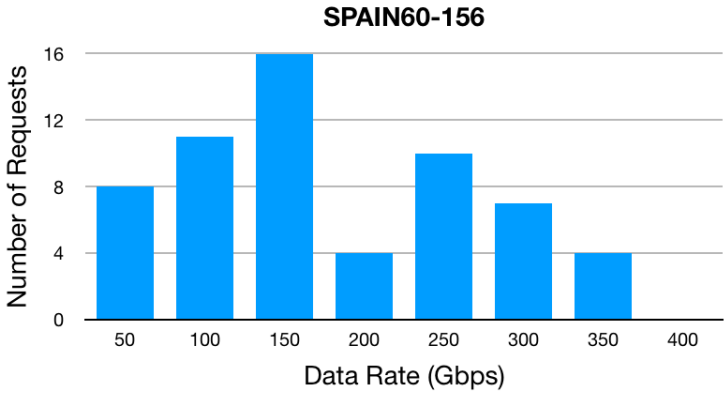

Figure A.9: Requests Distribution of RMSA Dataset SPAIN60-156.

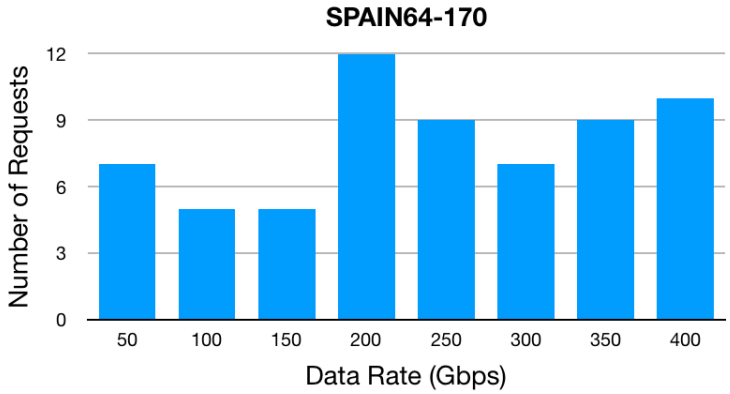

Figure A.10: Requests Distribution of RMSA Dataset SPAIN64-170.

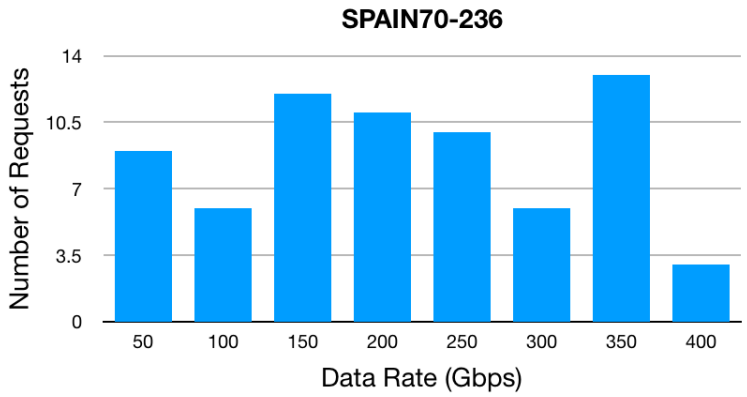

Figure A.11: Requests Distribution of RMSA Dataset SPAIN70-236.

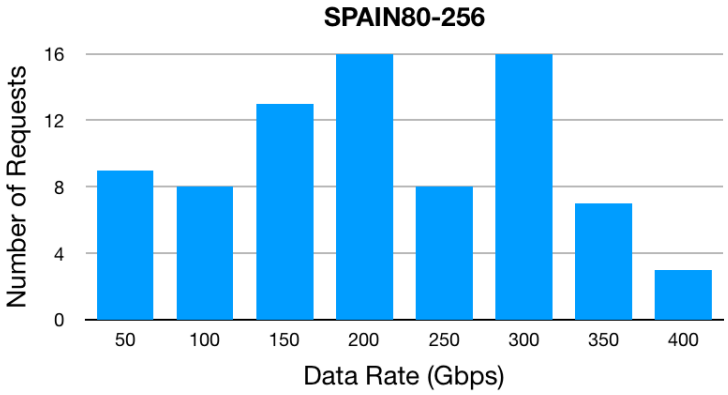

Figure A.12: Requests Distribution of RMSA Dataset SPAIN80-256.

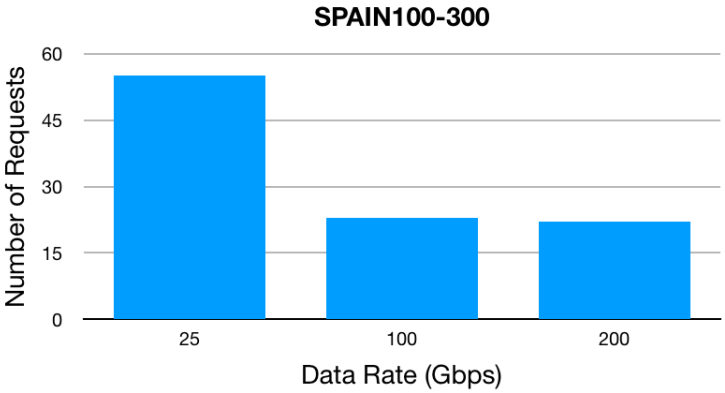

Figure A.13: Requests Distribution of RMSA Dataset SPAIN100-300.

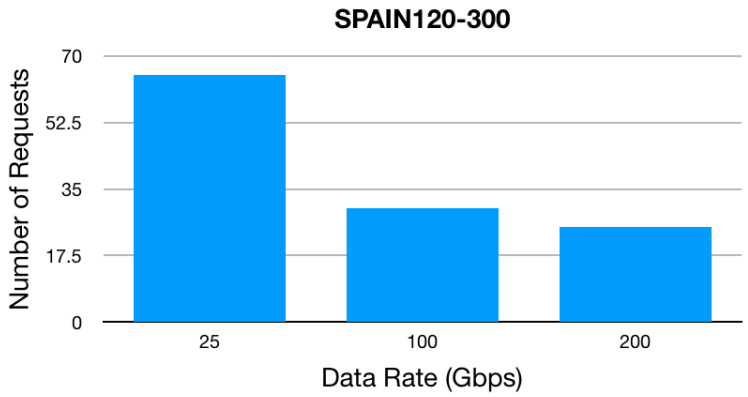

Figure A.14: Requests Distribution of RMSA Dataset SPAIN120-300.

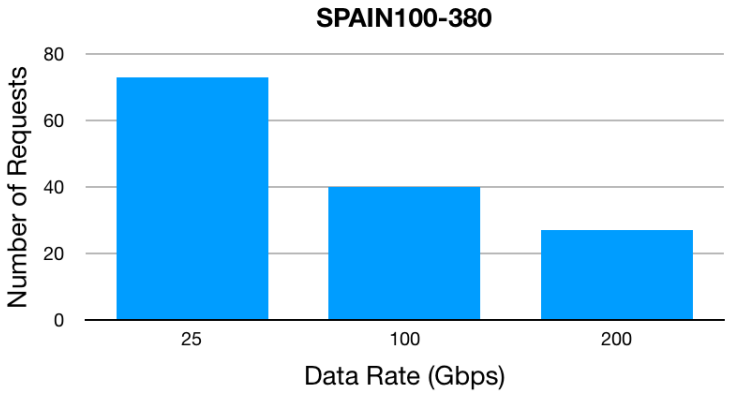

Figure A.15: Requests Distribution of RMSA Dataset SPAIN140-380A.

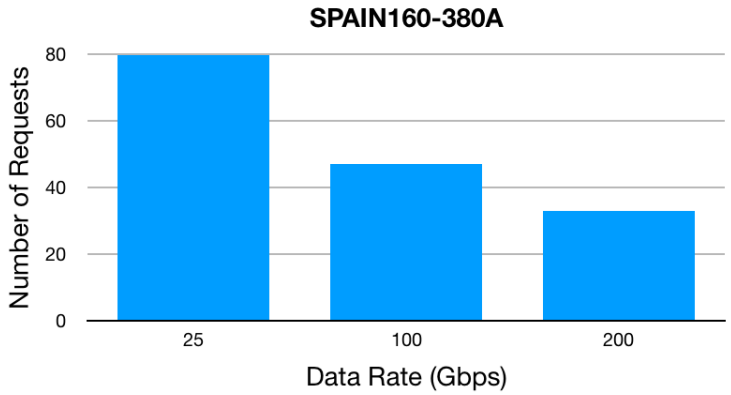

Figure A.16: Requests Distribution of RMSA Dataset SPAIN160-380A.

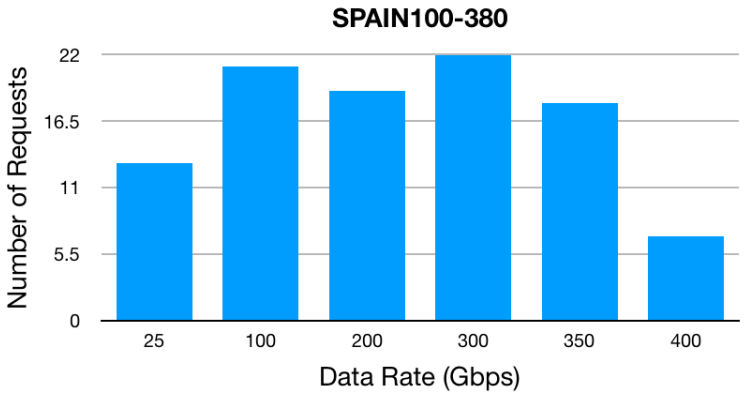

Figure A.17: Requests Distribution of RMSA Dataset SPAIN100-380.

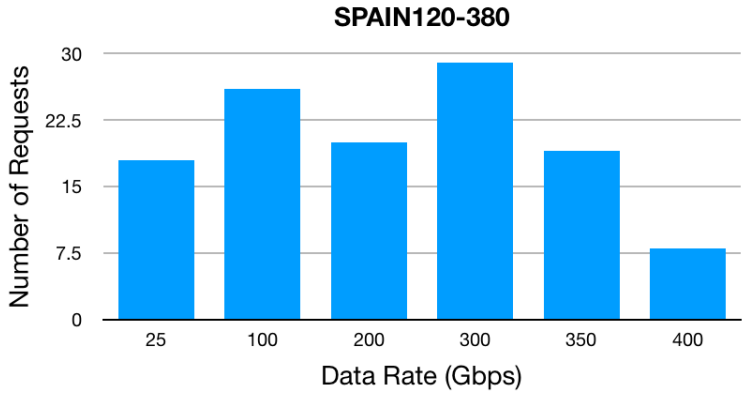

Figure A.18: Requests Distribution of RMSA Dataset SPAIN120-380.

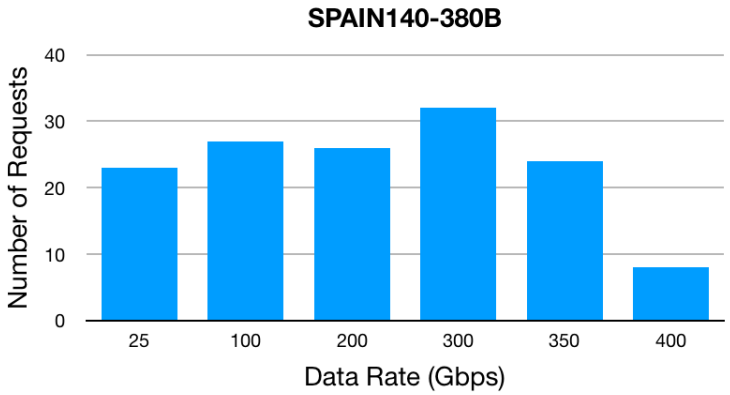

Figure A.19: Requests Distribution of RMSA Dataset SPAIN140-380B.

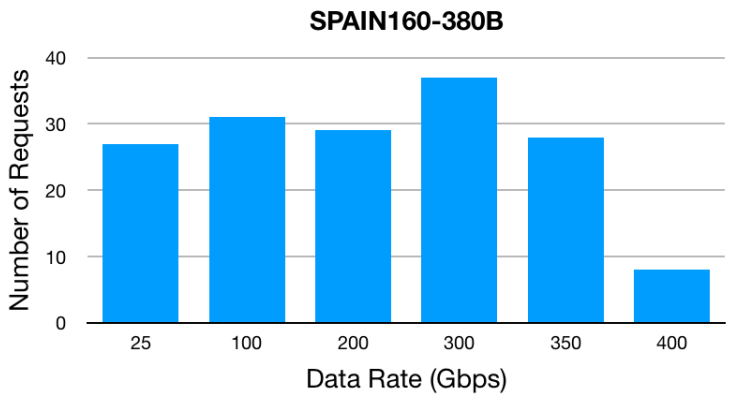

Figure A.20: Requests Distribution of RMSA Dataset SPAIN160-380B.

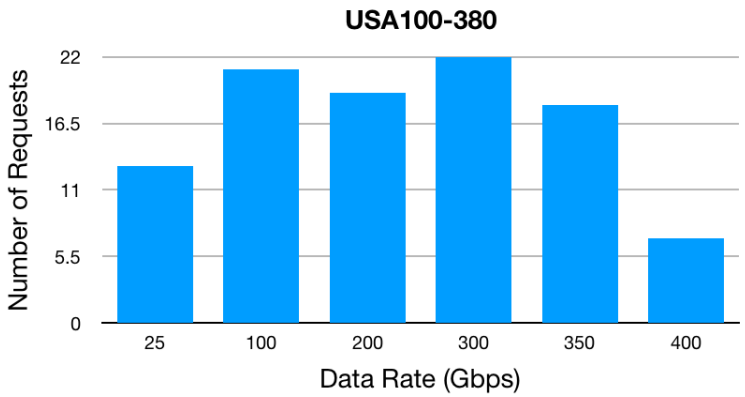

Figure A.21: Requests Distribution of RMSA Dataset USA100-380.

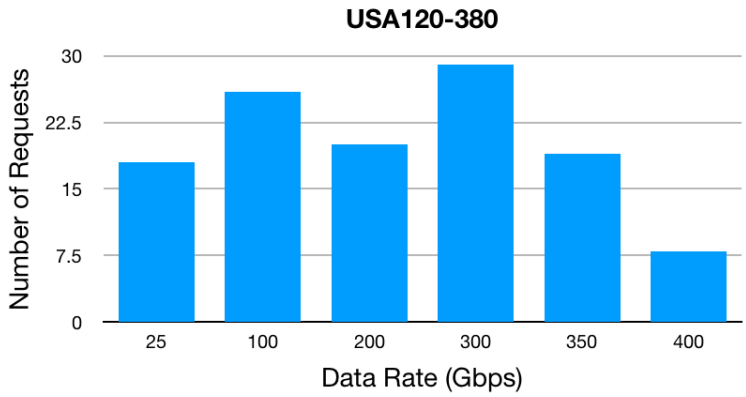

Figure A.22: Requests Distribution of RMSA Dataset USA120-380.

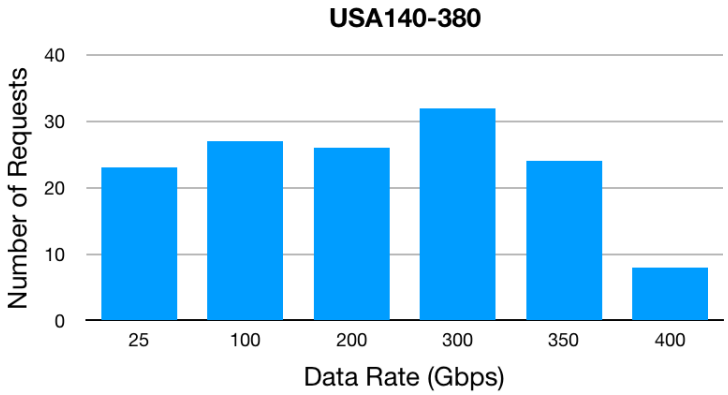

Figure A.23: Requests Distribution of RMSA Dataset USA140-380.

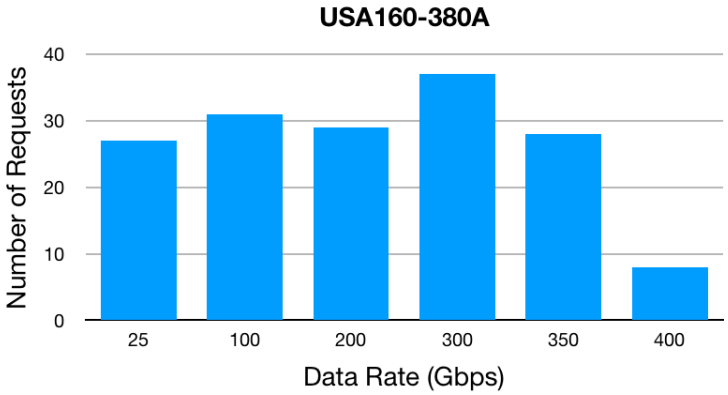

Figure A.24: Requests Distribution of RMSA Dataset USA160-380A.

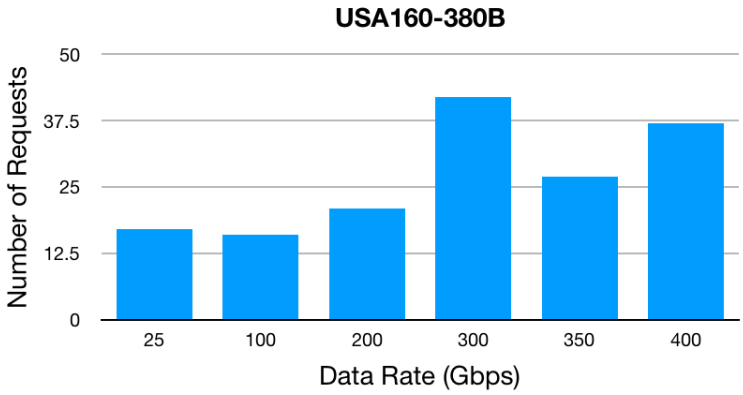

Figure A.25: Requests Distribution of RMSA Dataset USA160-380B.

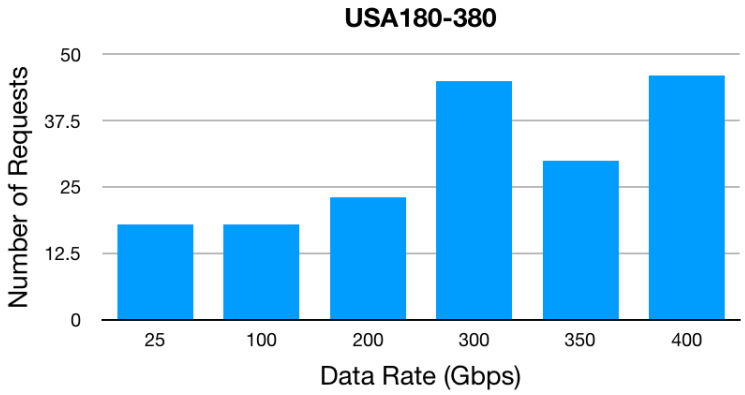

Figure A.26: Requests Distribution of RMSA Dataset USA180-380.

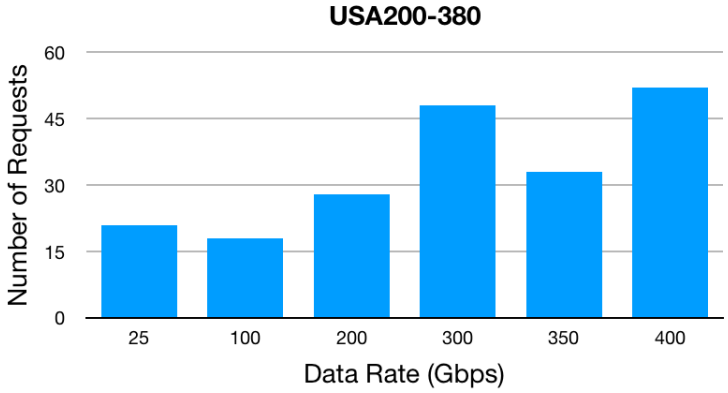

Figure A.27: Requests Distribution of RMSA Dataset USA200-380.

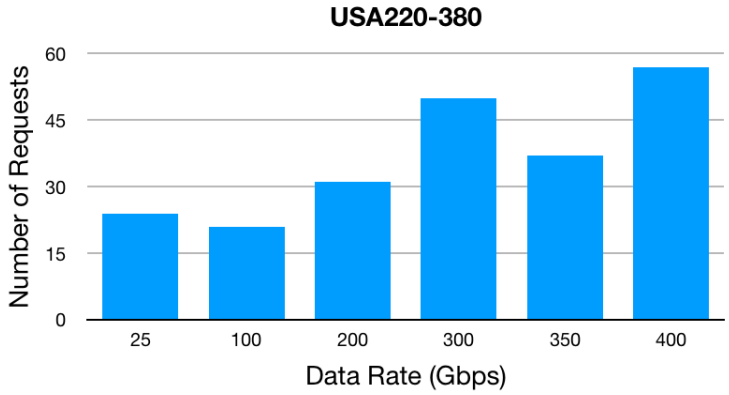

Figure A.28: Requests Distribution of RMSA Dataset USA220-380.

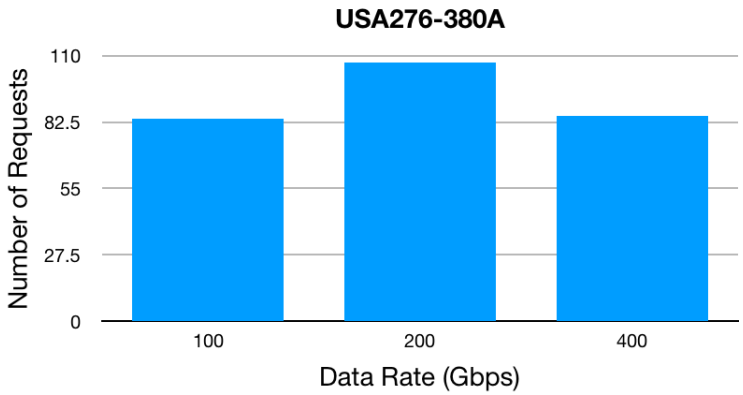

Figure A.29: Requests Distribution of RMSA Dataset USA276-380A.

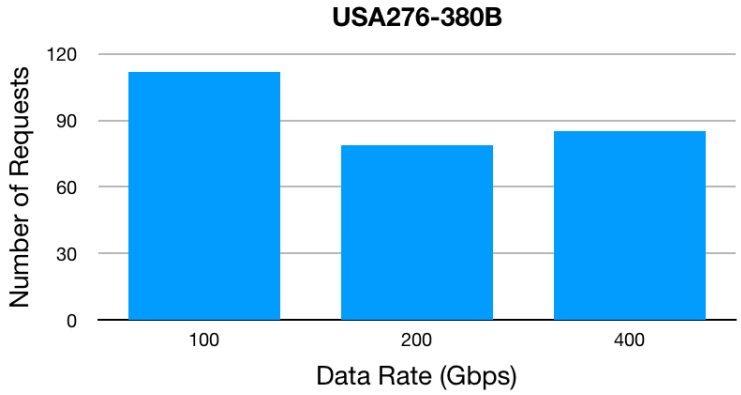

Figure A.30: Requests Distribution of RMSA Dataset USA276-380B.

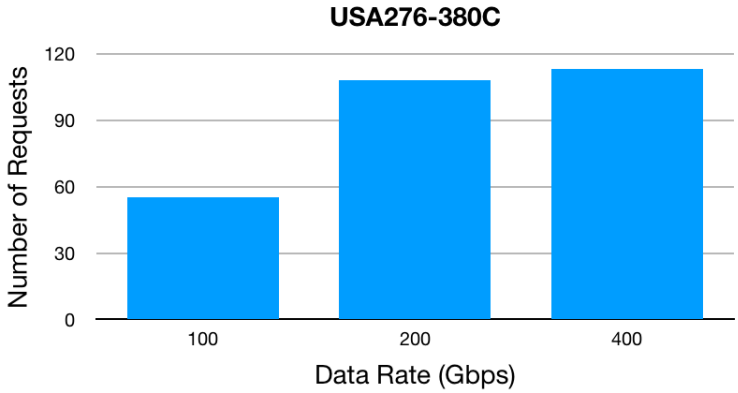

Figure A.31: Requests Distribution of RMSA Dataset USA276-380C.

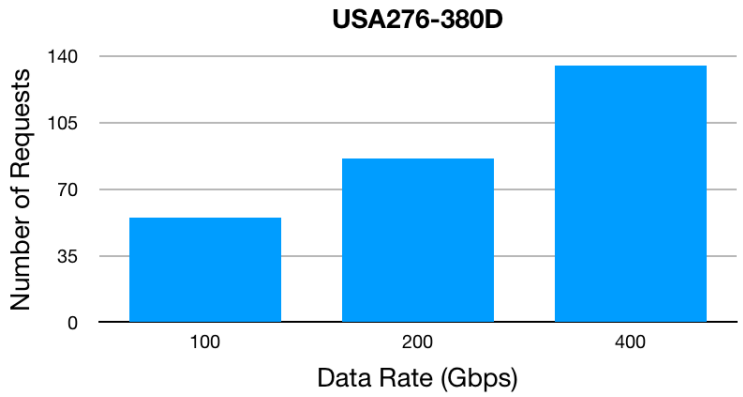

Figure A.32: Requests Distribution of RMSA Dataset USA276-380D.

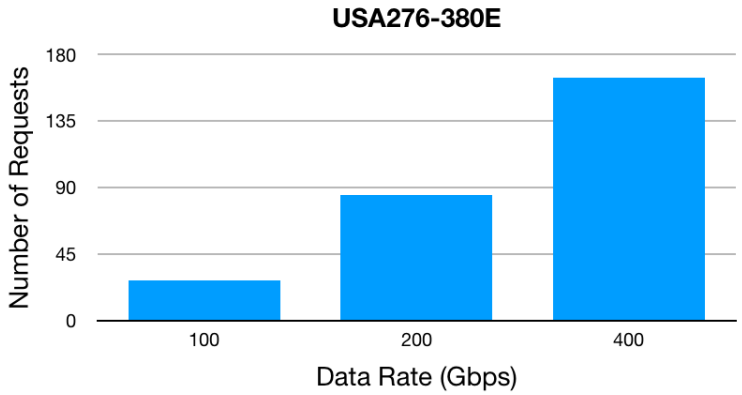

Figure A.33: Requests Distribution of RMSA Dataset USA276-380E.

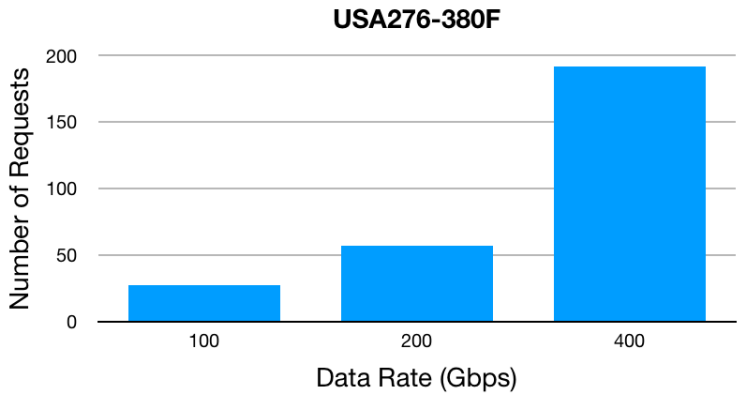

Figure A.34: Requests Distribution of RMSA Dataset USA276-380F.

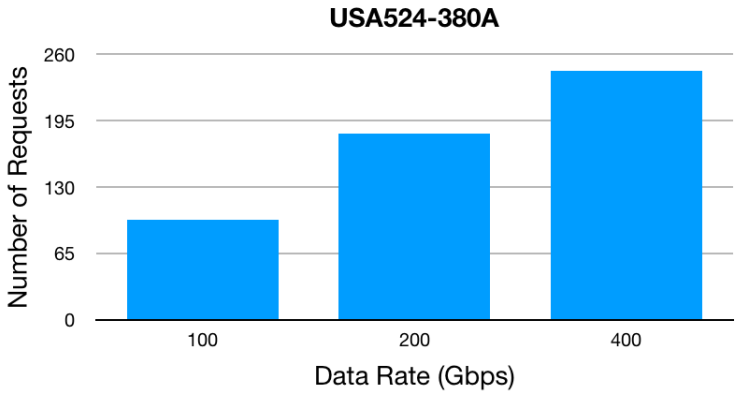

Figure A.35: Requests Distribution of RMSA Dataset USA524-380A.

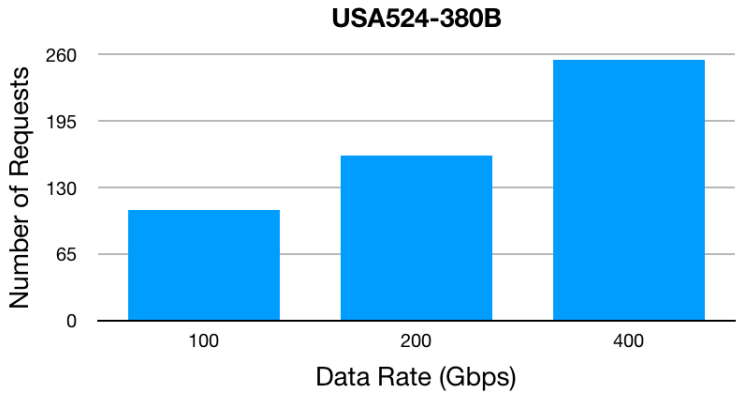

Figure A.36: Requests Distribution of RMSA Dataset USA524-380B.

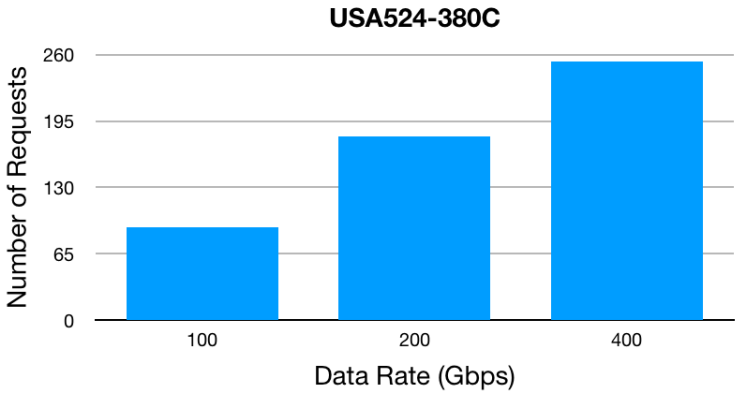

Figure A.37: Requests Distribution of RMSA Dataset USA524-380C.

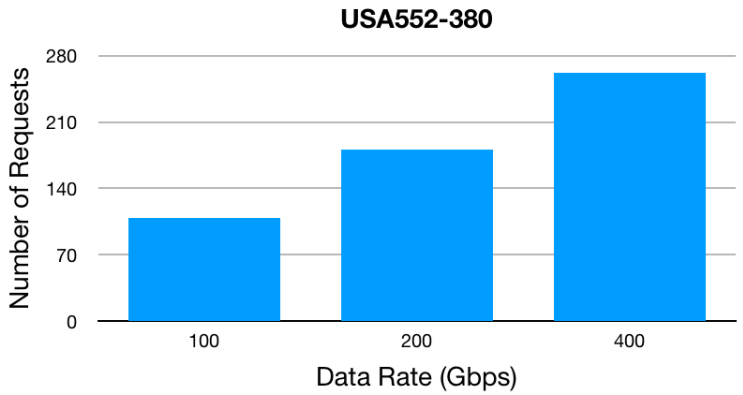

Figure A.38: Requests Distribution of RMSA Dataset USA552-380.

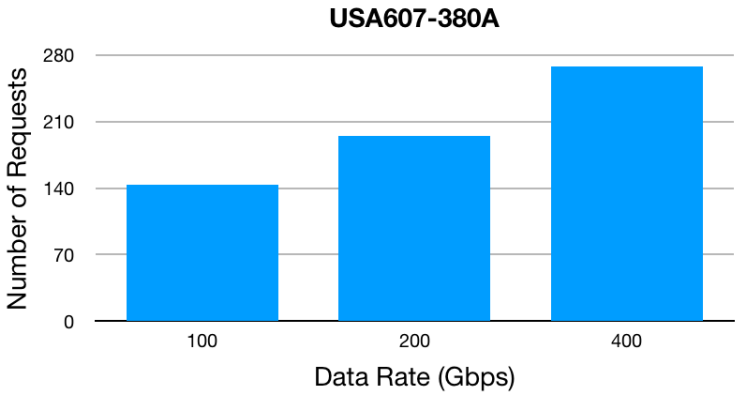

Figure A.39: Requests Distribution of RMSA Dataset USA607-380A.

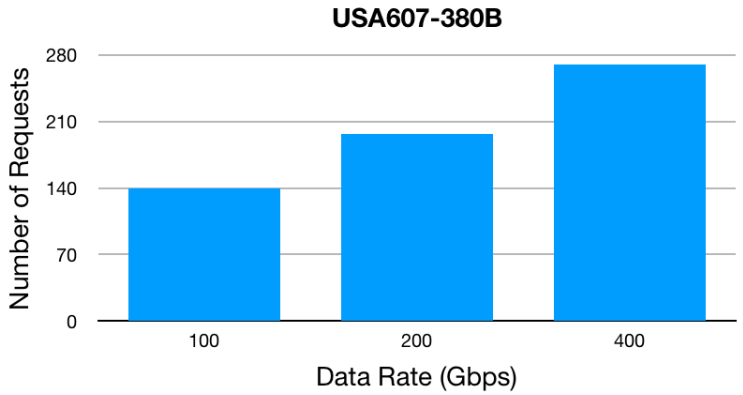

Figure A.40: Requests Distribution of RMSA Dataset USA607-380B.

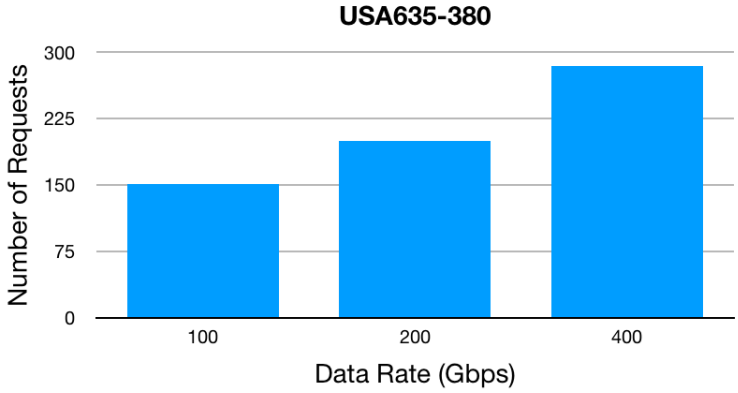

Figure A.41: Requests Distribution of RMSA Dataset USA635-380.

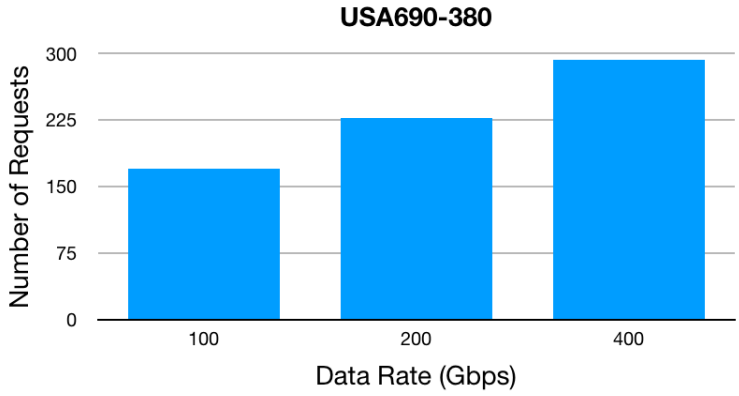

Figure A.42: Requests Distribution of RMSA Dataset USA690-380.